International Journal of Heat and Mass Transfer 171 (2021) 121060

Contents lists available at ScienceDirect

International Journal of Heat and Mass Transfer

journal homepage: www.elsevier.com/locate/hmt

Review

Assessment of void fraction models and correlations for subcooled boiling in vertical upflow in a circular tube

Chang Cai[a,b], Issam Mudawar[b,*], Hong Liu[a], Xi Xi[a]

[a] Key Laboratory of Ocean Energy Utilization and Energy Conservation of Ministry of Education, School of Energy and Power Engineering, Dalian University of Technology, Dalian, 116024, PR China
[b] Purdue University Boiling and Two-Phase Flow Laboratory (PU-BTPFL), School of Mechanical Engineering, 585 Purdue Mall, West Lafayette, IN 47907, USA

ARTICLE INFO

Article history:
Received 21 November 2020
Revised 24 January 2021
Accepted 2 February 2021
Available online 23 February 2021

Keywords:
Subcooled flow boiling
Void fraction
Net vapor generation
Vapor quality
Thermodynamic equilibrium quality

ABSTRACT

This paper provides a comprehensive review as well as assessment of accuracy of published models and correlations for net vapor generation point, vapor quality, and void fraction in subcooled vertical upflow boiling in a circular tube. Also provided is a detailed discussion on the rationale and physical mechanisms upon which the individual predictive methods are based. The assessment is accomplished by comparing predictions to a new consolidated database consisting of 61 data points for thermodynamic equilibrium quality at the net vapor generation point, amassed from 5 sources, and 1118 data points for void fraction, from 11 sources. Overall, it is shown that correlations by Saha and Zuber provide best predictions for both thermodynamic equilibrium quality at the point of net vapor generation and axial distribution of vapor quality. In terms of void fraction prediction, best accuracy among prior predictive methods is achieved, in order, using a slip ratio model by Thom, drift-flux model by Dix, slip ratio model by Ahmad, and modified homogeneous model by Nishino and Yamazaki. It is shown that the vast majority of models and correlations show far better accuracy over the higher range of void fraction of 0.20-1.0 than the low range of 0-0.2. A new and simple void fraction correlation spanning the entire range of flow conditions of the consolidated database is proposed, which is shown to yield superior overall predictive accuracy compared to prior models and correlations. Finally, a step-by-step procedure for calculating void fraction with best accuracy is presented.

1. Introduction

1.1. Fundamentals of subcooled flow boiling

Subcooled flow boiling is encountered in numerous industrial applications, such as steam generators, nuclear reactors, refrigeration systems, and chemical processing plants, as well as in thermal management of computer data centers and hybrid vehicle power electronics [1,2]. Accurate modeling of subcooled boiling is highly dependent on the ability to determine interfacial behavior and void fraction; this is crucial not only for flow boiling in tubes but other configurations as well, such as two-phase capillary flow [3], pool boiling [4], jet impingement [5], and spray [6]. And, because of recent increasing interest in cooling of high-power-density electronic devices and systems, investigators are now placing special emphasis on investigating both interfacial behavior and void fraction in mini/micro-channel flows [7,8].

Subcooled flow boiling is initiated with a single-phase liquid region at the inlet wherein the mean liquid temperature increases gradually in the axial direction in response to an applied heat flux. Using the commonly adopted assumption of thermodynamic equilibrium, vapor is postulated to begin forming at the axial location from the inlet corresponding to zero thermodynamic equilibrium quality ($x_e = 0$). However, in practical terms, the vapor will begin forming upstream of this location despite the bulk liquid remaining below saturation temperature, provided the wall temperature sufficiently exceeds the saturation temperature to permit vapor formation at the wall. The location where the first bubbles appear is the point of *onset of nucleate boiling* (ONB) [9], but, in highly subcooled boiling, the region immediately following ONB does not contribute any appreciable increase in vapor void fraction, given that bubbles in this region are subjected to a high degree of condensation. Farther downstream, as the bulk liquid temperature continues to rise, the degree of bulk subcooling gradually diminishes, which weakens the condensation effects, causing the wall bubbles to grow bigger and begin departing into the bulk flow, thereby allowing for

Abbreviations: HTC, heat transfer coefficient; MAE, mean absolute error; NVG, net vapor generation; ONB, onset of nucleate boiling; OSV, onset of significant void.

* Corresponding author.
E-mail address: mudawar@ecn.purdue.edu (I. Mudawar).

https://doi.org/10.1016/j.ijheatmasstransfer.2021.121060
0017-9310/

Nomenclature

A	flow area
A_1, A_2	parameter defined in Table 2
a	parameter defined in Table 1
Bo	boiling number
Bo^*	parameter defined in Table 2
b	parameter defined in Table 3
C	distribution parameter
C_i	parameter defined in Table 3 (i = 1-7)
c_p	specific heat at constant pressure
D	tube diameter
D_b	parameter defined in Table 2
E	parameter defined in Table 2
F	parameter defined in Table 1
f	parameter defined in Table 1
G	mass velocity
g	gravity
h	heat transfer coefficient; enthalpy
h'	parameter defined in Table 1
h_{fg}	latent heat of vaporization
K, K'	parameters defined in Table 3
K_0, K_1	parameters defined in Table 3
k	thermal conductivity
m	empirical parameter
m_1, m_2	parameters defined in Table 3
N	parameter defined in Table 3
n	number of datapoints
Pe	Peclet number
Pr	Prandtl number
p	pressure
q"	heat flux
Re	Reynolds number
r	parameter defined in Table 3
S	slip ratio
s	parameter defined in Table 3
s_i	parameter defined in Eq. (8) (i = 1-4)
T	temperature
u	velocity
u^*	parameter defined in Table 1
u_{gj}	drift velocity
W	mass flux
We	Weber number
X_{tt}	Lockhart-Martinelli parameter
x	flow quality
x_e	thermodynamic equilibrium quality
Y	parameter defined in Table 3
Y^+	parameter defined in Table 1
y	parameter defined in Table 2
z	distance from tube inlet

Greek symbols

α	void fraction
ε	parameter defined in Table 3
μ	viscosity
ν	kinetic viscosity
ξ	parameter defined in Table 2
ρ	density
σ	surface tension
φ	parameter defined in Table 3
χ	universal parameter in Eq. (7)

Subscripts

c	critical point
exp	experimental (measured)
f	liquid
g	vapor
H	homogenous model
in	inlet
NVG	net vapor generation
pred	predicted
sat	saturated
sp	single-phase
sub	subcooling

a measurable increase in void fraction. The axial location where the void fraction begins to incur such an increase is referred to as point of *net vapor generation* (NVG) or, synonymously, *onset of significant void* (OSV) [9]. A common demarcation of subcooled boiling flow regions is: (i) *single-phase liquid region* upstream of the axial location of ONB, (ii) two-phase *highly subcooled region* between the axial locations of ONB and NVG, (iii) *slightly subcooled region* between the axial locations of NVG and $x_e = 0$, and (iv) *saturated boiling region* beginning at the location of $x_e = 0$. Clearly, the void fraction trends vary greatly among these regions.

Subcooled flow boiling is influenced by several factors, including inlet pressure, inlet subcooling, mass velocity, heat flux, flow orientation, and tube shape and hydraulic diameter, let alone the thermophysical properties of the working fluid. The lack of thermodynamic equilibrium between the vapor and liquid phases is cause for great difficulty modeling interfacial behavior and predicting void fraction in subcooled boiling. A useful reference for exploring two-phase behavior in subcooled boiling is local thermodynamic equilibrium quality, which is defined as

$$x_e = \frac{h - h_{f,sat}}{h_{fg}}, \tag{1}$$

where h, $h_{f,sat}$, and h_{fg} are, respectively, the local enthalpy, saturated liquid enthalpy, and latent heat of vaporization. The thermodynamic equilibrium quality is in effect a measure of the degree of deviation from saturation. For a uniformly heated circular tube, the local thermodynamic equilibrium quality can be calculated using a simple energy balance,

$$x_e = \frac{\frac{4q''z}{GD} + h_{in} - h_{f,sat}}{h_{fg}} \tag{2}$$

where h_{in}, q'', G, D and z, are, respectively, the liquid inlet enthalpy, wall heat flux, mass velocity, tube diameter, and axial distance from the inlet.

1.2. Void fraction in subcooled flow boiling

Knowledge of void fraction in subcooled flow boiling is of considerable practical importance in virtually any two-phase flow calculation because it is indispensable to the prediction of several other two-phase parameters, such as thermophysical properties, pressure drop, heat transfer coefficient, and critical heat flux. Moreover, void fraction plays a crucial role when characterizing flow regime transitions in subcooled flow boiling.

Void fraction refers to the ratio of space occupied by the vapor to the total space within the flow tube. As discussed in [10], there are four commonly used definitions for void fraction: *local, chordal, cross-sectional* and *volumetric*, which refer to ratios based on point, line, plane, and volume, respectively. The average cross-sectional void fraction, α, defined as ratio of the portion of cross-sectional area occupied by vapor, A_g, to the total cross-sectional area, A, is the most frequently used definition, and is also adopted in the present study. It is obvious that the magnitude of void fraction is

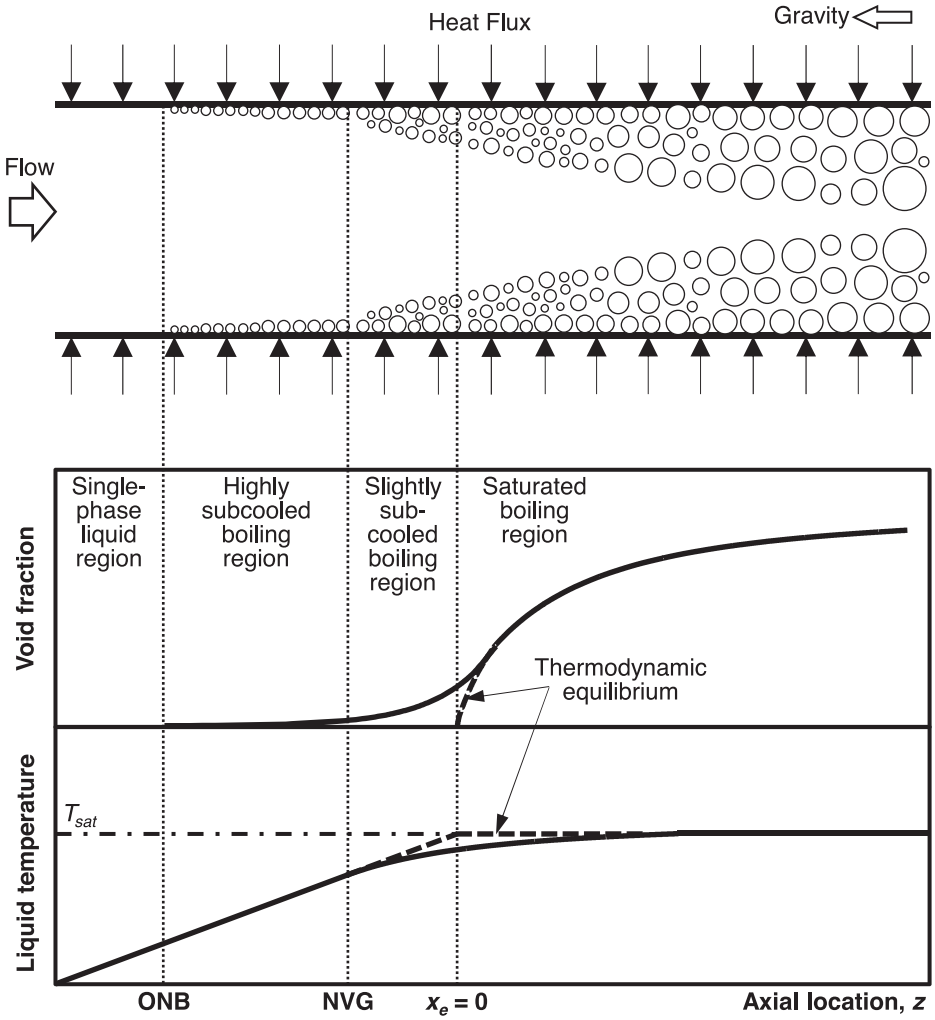

Fig. 1. Schematic of void fraction evolution in subcooled flow boiling.

bounded between 0, corresponding to pure liquid, and unity, corresponding to pure vapor.

Fig. 1 shows a schematic of the axial distribution of void fraction in subcooled flow boiling. Only liquid exists in the single-phase liquid region extending from the tube inlet to the ONB point, within which $\alpha = 0$. At the ONB point, vapor bubbles begin to form, but in the highly subcooled region just downstream of ONB, the bubbles remain attached to or slide along the heated wall and tend to quickly condense and/or collapse because of the highly subcooled liquid core. Therefore, the void fraction within this region exhibits a very mild and slow steam-wise increase. The NVG point marks the axial location where a noticeable increase in void fraction begins to take effect. This is where the bulk liquid subcooling decreased to a level where vapor condensation effects are suppressed, and vapor bubbles begin to grow and depart from the wall. The NVG point marks a transition between the highly subcooled region and slightly subcooled region. The void fraction continues to increase downstream of the location of $x_e = 0$ corresponding to the saturated boiling region.

Due to the complexity in treating thermodynamic non-equilibrium effects in subcooled flow, predicting void fraction in a purely theoretical manner is a formidable challenge. This is why most published void fraction relations follow purely empirical or semi-empirical formulations, relying heavily on idealizations of underlying interfacial behavior and fitting of empirical coefficients. As will be discussed in subsequent sections, comparatively successful relations show reasonable agreement with experimental data only within their own validity range. A robust and accurate method to predicting the void fraction, with a broad application range, is still lacking and therefore warrants careful further study.

As to experimental studies, various techniques have been developed for measuring void fraction in two-phase flow, which can be classified as intrusive or non-intrusive. The former methods, including wire mesh tomography [11,12], optical fiber probe sensors [13,14], impedance sensors [15,16], hot-film anemometry [17], and quick closing valves [18,19], undoubtedly create disturbances to the flow, especially for small channels. On the other hand, non-intrusive techniques provide superior measurement accuracy. They include photon [20], neutron [21], x-ray [11,22] and γ-ray [23,24] attenuation methods, ultrasonic wave propagation sensors [25,26], capacitive sensors [27,28], and direct visualization using high-speed cameras [29]. However, most non-intrusive techniques pose important challenges, including high cost and safety [30], and only transparent glass tubes can be used when adopting optical techniques, which limits their ability to tackle flow in practical metallic tubes.

1.3. Objectives of present study

Several review articles have been published in the past which examined void fraction in vertical upflow. They can be classified into four categories: (1) adiabatic gas-liquid two-phase flow

in tubes [31–35], (2) diabatic steam-liquid two-phase flow in rod bundles [36–38], (3) diabatic steam-liquid two-phase flow in tubes, and (4) combination of different flow orientations and configurations [39–43]. The third group (*i.e.*, reviews dedicated exclusively to subcooled upflow boiling in vertical tubes) includes works by Chexal *et al.* [44] and Vijayan *et al.* [45,46], in which data for rectangular and annular channels were also examined.

The present study will first provide a comprehensive summary of underlying mechanisms and predictive methods for the NVG point, which corresponds to the onset of increasing void fraction. This will be followed by a review of vapor quality and void fraction relations for two-phase upflow in a vertical circular tube. To assess the accuracy of these relations, a consolidated experimental database is amassed from 11 sources, which consists of 1118 data points for void fraction spanning broad ranges of inlet pressure, inlet subcooling, tube diameter, mass velocity, and heat flux. Based on this assessment, the most accurate predictive methods are identified and recommended for prediction of (1) thermodynamic equilibrium quality at the NVG point, $x_e|_{NVG}$, (2) vapor quality, x, and (3) void fraction, α, which include a new and both simple and accurate correlation for void fraction.

2. Predictive methods for point of net vapor generation (NVG)

Kroeger and Zuber [47] proposed that reliable determination of location of the NVG point is essential to accurate prediction of axial variation of vapor void fraction in subcooled flow boiling. Since void fraction is negligibly small between ONB and NVG, it is assumed for simplicity in the present study (as well as majority of prior studies) that, rather than the ONB point, the NVG point is the effective starting point for void fraction initiation. In other words, the heated tube is demarcated by the NVG point into single-phase and two-phase regions. In this section, prior predictive methods for the NVG point will be briefly reviewed.

While the vast majority of studies agree that the NVG point is the location corresponding to the onset of increasing void fraction, and that its occurrence depends only on local thermal parameters and flow conditions, there is a lack of concesus regarding the trigger mechanism for NVG. Overall, NVG point relations can be categorized into one of three groups according to the mechanism proposed: (1) *thermal/hydrodynamic*, (2) *bubble departure*, and (3) *bubble ejection*, which will be discussed briefly.

2.1. Thermal/hydrodynamic mechanism

The relations proposed by Griffith [48], Ahmad [49], Saha and Zuber [50] and Ünal [51] all fall into this thermal/hydrodynamic category, to name a few. But these relations differ in their description of the physical mechanism responsible for initiating the NVG condition, though they all share the notion that the NVG point is the outcome of near wall conditions dictated by local heat transfer effects. For example, Griffith [48] suggested that the NVG point is the location where the heated surface becomes fully covered with a layer of attached bubbles, rendering the vapor layer ripe for a substantial increase in the vapor production. Another hypothesis is based on comptetion between the rates of vapor generation by boiling versus condensation [52] in which the NVG point is viewed a transition condition where the former just begins to exceed the later. And, downstream the NVG point, the same hypotehis points to the boiling greatly overwhelming the condensation, which causes the observed appreciable increase in the vapor production. Another hypothesis, proposed by Ahmadi and Okawa [53] based on experimental results for subcooled flow boiling in a vertical rectangular tube, is that the NVG point occurs at the axial location where the liquid subcooling equals the wall superheat.

Among the published thermal/hydrodynamic models, Saha and Zuber [50] is by far the most widely used. This hypothesis is based on the assumption that the NVG point is controlled thermally at low mass velocities and hydrodynamically at high mass velocities, with the transition between the two regimes occurring at a Peclet number ($Pe = Re.Pr_f$) of 70,000. Lee and Bankoff [54] showed the Saha and Zuber correlation is among the most accurate tools available for predicting the NVG point. Additionally, several subsequent investigators adopted the same form of the Saha and Zuber model to correlate their own NVG data [55-58].

2.2. Bubble departure mechanism

Other studies attribute the point of NVG to the ability of bubbles to begin departing from the heated wall. According to this mechanism, bubbles are very small and remain attached to or slide along the wall between the ONB and NVG points, with the latter providing the first opportunity for bubble departure.

One example of formulations utilizing this hypothesis is work by Levy [59], who proposed that a bubble would depart from the heated wall when the shear and buoyancy forces combined just exceed the surface tension force. A key advantage of Levy's formulation is minimal reliance on empiricism, as well as ability to be further extended to account for effects of contact angle and surface roughness [60–62]. On the other hand, data and observations from subsequent experimental works contradict the assumptions of the Levy formulation [63–65], which explains why this hypothesis has lost popularity in recent years.

2.3. Bubble ejection mechanism

A key difference between the mechanisms of bubble departure and bubble ejection is that, while both are based on a bubble force balance, the former is based on forces along the flow direction, while that latter considers forces perpendicular to wall.

Dix [66] proposed a mechanism relating the occurrence of the NVG point to the ability of bubbles to be ejected from a heated wall bubbly layer. He postulated that, because of thermocapillary and wall vortex effects, vapor bubbles in the highly subcooled region cannot detach from the heated wall and end up forming a wall bubbly layer. But, once the bubbly layer thickness exceeds a threshold value, the bubble growth becomes unstable, causing the bubbles to be ejected into the liquid core. They concluded this destabilization of the bubbly layer is a primary cause for the observed rapid increase in vapor void at the NVG point [67].

However, subsequent flow visualization studies showed that bubble ejection sometimes begins some distance upstream of the NVG point, even immediately downstream of the ONB point [64,68], therefore diputing the validity of the bubble ejection mechanism.

Overall, a key target for most studies aimed at predicting location of the NVG point in subcooled flow boiling is to determine the corresponding thermodynamic equilibirum quality, $x_e|_{NVG}$. A summary of the $x_e|_{NVG}$ models and correlations is provided in Table 1, along with corresponding ranges of operating conditions for each. Missing ranges of operating conditions for certain models and correlations is rooted in the lack of availability of such information in many studies. Quite often, the relations proposed in one study are extracted from previously published articles with no mention of relevant operating conditions.

Given the lack of models and correlations providing broad coverage of operating conditions, a common practice has been to extrapolate relations beyond their applicability range, which can clearly lead to serious predictive errors.

Table 1
Summary of models and correlations for thermodynamic equilibirum quality corresponding to the NVG point, $x_e|_{NVG}$, in subcooled flow boiling.

Author(s)	Formulae	Remarks
Griffith *et al.* [48] (1958)	$x_{e,NVG} = -\frac{q''\rho_f c_{pf}}{Gh_{fg}}\frac{14+0.1p}{100}$	p is in atm, u_{in} = 6.1-9.1 m/s, p = 3.5-10.3 MPa, $\Delta T_{sub,in}$ = 5-83 K, q'' = 18-120 W/cm^2, G = 6000-9000 kg/m^2.s
Levy [59] (1967)	$x_{e,NVG} = \begin{cases} -\frac{q''}{h_{fg}}\left(\frac{c_{pf}}{h_{sp}} - \frac{\Pr_f Y^+}{G\sqrt{f/8}}\right), Y^+ \le 5 \\ -\frac{q''}{h_{fg}}\left\{\frac{c_{pf}}{h_{sp}} - \frac{5}{G\sqrt{f/8}}[\Pr_f + \ln(1+\frac{\Pr_f Y^+}{5} - \Pr_f)]\right\}, 5 < Y^+ \le 30 \\ -\frac{q''}{h_{fg}}\left\{\frac{c_{pf}}{h_{sp}} - \frac{5}{G\sqrt{f/8}}[\Pr_f + \ln(1+5\Pr_f) + 0.5\ln(\frac{Y^+}{30})]\right\}, Y^+ > 30 \end{cases}$	$h_{sp} = 0.023\frac{k_f}{D}(\frac{GD}{\mu_f})^{4/5}(\frac{c_{pf}\mu_f}{k_f})^{2/5}$, $Y^+ = 0.015\sqrt{\sigma D\rho_f}/\mu_f$, $f = 0.0055[1+(2+\frac{10^6}{\mathrm{Re}})^{1/3}]$
Ahmad [49] (1970)	$x_{e,NVG} = -\frac{q''c_{pf}D}{2.44k_f h_{fg}}(\frac{GD}{\mu_f})^{-1/2}(\frac{c_{pf}\mu_f}{k_f})^{-1/3}(\frac{h_{in}}{h_f})^{-1/3}(\frac{h_{fg}}{h_f})^{-1/3}$	p = 1-13 MPa, G = 130-1450 kg/m^2.s, q'' = 30-120 W/cm^2
Dix [66] (1971)	$x_{e,NVG} = -0.00135\frac{q''}{h_{sp}}\frac{c_{pf}}{h_{fg}}(\frac{GD}{k_f\mu_f})^{1/2}$	
Saha & Zuber [50] (1974)	$x_{e,NVG} = \begin{cases} -0.0022\frac{q''c_{pf}D}{h_{fg}k_f}, Pe < 70000 \\ -153.85\frac{q''}{h_{fg}G}, Pe > 70000 \end{cases}$	p = 0.101-13.8 MPa, G = 400-1050 kg/m^2.s, q'' = 2.0-121 W/cm^2; both circular and rectangular tubes
Ünal [51] (1975)	$x_{e,NVG} = \frac{aq''}{h_{sp}}\frac{c_{pf}}{h_{fg}}$, where $a = \begin{cases} -0.11, u_f < 0.45\text{m/s} \\ -0.24, u_f \ge 0.45\text{m/s} \end{cases}$ for water and $a = \begin{cases} -0.11, u_f < 0.45\text{m/s} \\ -0.18, u_f \ge 0.45\text{m/s} \end{cases}$ for R22; h_{sp} is single-phase HTC	p = 0.1-15.8 MPa, G = 132-2818 kg/m^2.s, q'' = 2.0-192 W/cm^2, $\Delta T_{sub,in}$ = 3.2-42 K; circular, rectangular and annular tubes
Sekoguchi *et al.* [69] (1980)	$x_{e,NVG} = -13.5(\frac{q''}{Gh_{fg}})^{0.65}$	p = 0.1-14.06 MPa, G = 130-5097 kg/m^2.s, q'' = 1.86-380 W/cm^2; circular, rectangular and annular tubes
Siman-Tov *et al.* [70] (1995)	$x_{e,NVG} = \begin{cases} -0.0022(0.55+11.21/\Delta T_{sub,in})\frac{q''c_{pf}D}{h_{fg}k_f}, Pe < 70000 \\ -153.85(0.55+11.21/\Delta T_{sub,in})\frac{q''}{h_{fg}G}, Pe > 70000 \end{cases}$	
Kataoka *et al.* [71] (1997)	$x_{e,NVG} = \begin{cases} -0.0022\frac{q''c_{pf}D}{h_{fg}k_f}\frac{q''}{8800}, Pe < 70000 \\ -153.85\frac{q''}{h_{fg}G}\frac{q''}{8800}, Pe > 70000 \end{cases}$	q'' is in kW/m^2, p = 1.0-7.1 MPa, G = 500-2000 kg/m^2.s; low heat flux and low subcooling conditions
Kalitvianski [72] (2000)	$x_{e,NVG} = \begin{cases} -0.011\frac{q''c_{pf}D}{h_{fg}k_f}, Pe < 36400 \\ -26678.159\frac{q''c_{pf}D}{h_{fg}k_f Pe^{1.4}}, Pe > 36400 \end{cases}$	p = 4.4-11 MPa, Pe = 32000-311000, G = 340-2100 kg/m^2.s, q'' = 43-172 W/cm^2
Sun *et al.* [73] (2003)	$x_{e,NVG} = \frac{1-\sqrt{1+1.6\rho_f q''c_{pf}/\rho_g h_{fg}h'}}{2\rho_f/\rho_g}$, where $h' = \frac{k_f}{D_b}(\frac{\rho_g}{\rho_f})^{0.41}\Pr_f^{-1.2}(\frac{\rho_f u_{gj}D_b}{\mu_f})^{1/2}$, $u_{gj} = 1.41[\frac{g\sigma(\rho_f-\rho_g)}{\rho_f^2}]^{1/4}$, $D_b = [\frac{\sigma}{g(\rho_f-\rho_g)+0.75G^2/\rho_f D}]^{1/2}$	p = 1.2-2.3 MPa, G = 238-478 kg/m^2.s, q'' = 1.27-9.4 W/cm^2, $x_{e,in}$ = -0.61- -0.10; R12 in an annular tube
Ha *et al.* [55] (2005)	$x_{e,NVG} = \begin{cases} -\frac{q''c_{pf}DPe^{0.08}}{918.525h_{fg}k_f}, Pe < 52000 \\ -\frac{q''c_{pf}DPe^{-0.876}}{0.0287h_{fg}k_f}, Pe > 52000 \end{cases}$	new fit to data cited by Saha & Zuber [50]
Ha *et al.* [56] (2018)	$x_{e,NVG} = \begin{cases} -7.29(\frac{q''}{Gh_{fg}})^{0.8203}, u^* \le 1.55 \\ -32.94(\frac{q''}{Gh_{fg}})^{0.9016}, u^* > 1.55 \end{cases}$, where $u^* = \frac{G}{1.18\rho_f}[\frac{\rho_f^2}{g\sigma(\rho_f-\rho_g)}]^{0.25}$	p = 0.11-0.983 MPa, $Pe \le$ 70000, G = 65-635 kg/m^2.s, q'' = 9.7-118.6 W/cm^2, $\Delta T_{sub,in}$ = 11-86 K; circular and annular tubes
Ha *et al.* [57] (2019)	$x_{e,NVG} = \begin{cases} -\frac{q''c_{pf}D}{h_{fg}k_f}[0.0901 - 0.0893\exp(-\frac{158}{Pe})], u^* < 1.2 \\ -0.9176\frac{q''c_{pf}D}{h_{fg}k_f}Pe^{-0.5833}, u^* > 1.2 \end{cases}$, where $u^* = \frac{G}{1.53\rho_f}[\frac{\rho_f^2}{g\sigma(\rho_f-\rho_g)}]^{0.25}$	p = 0.11-6.9 MPa, Pe = 3600-329000, G = 65-2075 kg/m^2.s, q'' = 9.7-118.6 W/cm^2, $\Delta T_{sub,in}$ = 10-79 K; circular, rectangular and annular tubes
Ha *et al.* [58] (2020)	$x_{e,NVG} = \begin{cases} -\frac{q''c_{pf}D}{h_{fg}k_f}[0.0901 - 0.0893\exp(-\frac{158}{Pe})], u^* < 1.3 \\ -\frac{q''c_{pf}D}{h_{fg}k_f}\frac{\mathrm{Re}^{-0.77}\Pr^{-1.35}}{0.0959}, u^* > 1.3 \end{cases}$, where $u^* = \frac{G}{1.53\rho_f}[\frac{\rho_f^2}{g\sigma(\rho_f-\rho_g)}]^{0.25}$	p = 0.11-15 MPa, Pe = 3600-333000, G = 65-2532 kg/m^2.s, q'' = 9.7-221 W/cm^2, $\Delta T_{sub,in}$ = 10-163 K; circular, rectangular and annular tubes
SRL Model**	$x_{e,NVG} = \begin{cases} -0.0022\frac{q''c_{pf}D}{h_{fg}k_f}, Pe < 70000 \\ -\frac{1}{0.0055-0.0009F}\frac{q''}{h_{fg}G}, Pe > 70000 \end{cases}$	$F = \frac{1.0782}{1.015+\exp(\frac{p}{193032}-5.0268)}$

*From ref. [30]
**From ref. [56]

3. Predictive methods for vapor quality

Vapor quality, x, also termed 'mass dryness fraction' in some studies, is defined as the ratio of mass flow rate of vapor to the total flow rate,

$$x = \frac{W_g}{W_g + W_f} = \frac{\rho_g u_g A_g}{\rho_g u_g A_g + \rho_f u_f A_f} \tag{3}$$

where W, ρ, u, A are the mass flow rate, density, velocity, and flow area.

Ideally, the vapor quality is equal to the thermodynamic equilibrium quality, x_e, only under conditions of 'well mixed' equilibrium flow conditions. However, this not never the case for subcooled boiling, where the two-phase mixture (subcooled liquid and saturated or superheated vapor) exists in a thermodynamic nonequilibrium state. Under these conditions, x_e may be negative where x is positive. Similar to void fraction, x ranges from 0 to 1, and its value may be significantly different from that of x_e, the difference between x ***x***and x_e being an indicator of the degree of thermodynamic nonequilibrium.

As will be shown in the next section, void fraction, α, is generally expressed as a function of x, not x_e. Therefore, accurate prediction of void fraction requires use of appropriate relations for x as well. Table 2 provides a summary of published relations for x, include both mechanistically based and empirical functions of x_e and $x_e|_{NVG}$. Here too, missing ranges of operating conditions is rooted

Table 2
Summary of models and correlations for vapor quality, x, in subcooled flow boiling.

Author(s)	Formulae	Remarks
Bowring (1962)*	$x = \frac{1}{1+3.2\frac{\rho_f c_{pf}}{\rho_g h_{fg}}}[(x_e - x_{e,\mathrm{NVG}}) + \frac{h_{sp}h_{fg}}{2c_{pf}q''}(x_e - x_{e,\mathrm{NVG}})^2]$	q'' is in W/cm^2, $x_{e,\mathrm{NVG}}$ is calculated using relation by Griffith *et al.* [48]
Saha & Zuber [50] (1974)	$x = \frac{x_e - x_{e,\mathrm{NVG}}\exp(x_e/x_{e,\mathrm{NVG}}-1)}{1-x_{e,\mathrm{NVG}}\exp(x_e/x_{e,\mathrm{NVG}}-1)}$	
Sekoguchi *et al.* [69] (1980)	Method 1: $x = A_1\xi\exp(-A_2/\xi)$, where $\xi = (x_{e,\mathrm{NVG}} - x_e)/x_{e,\mathrm{NVG}}$, $A_1 = 4.4Bo\mathrm{Pr}^{2/3}\mathrm{Re}^{1/5}\exp(A_2)$, $A_2 = -0.0836x_{e,\mathrm{NVG}}Bo^{-1}\mathrm{Pr}^{-2/3}\mathrm{Re}^{-1/5}$ Method 2: Assume x' and calculate α, then calculate x'' as $x'' = Bo^*(\frac{2}{7}y^{9/7} - \frac{3}{35}y^{16/7})$, where $Bo^* = \frac{q''c_{pf}}{h_{fg}h'_{sp}}$, $h'_{sp} = \frac{k_f}{D}(\frac{GD}{\mu_f}\frac{1-x}{1-\alpha})^{4/5}(\frac{c_{pf}\mu_f}{k_f})^{2/5}$, $y = [\frac{5}{6}(1 + \frac{x_e}{Bo^*})]^7$. Repeat calculation until x' converges with x'', then $x = \begin{cases} x'', x_e < 0.2Bo^* \\ x_e, x_e \geq 0.2Bo^* \end{cases}$	

*From ref. [30]

in the lack of availability of such information from the indicated sources.

4. Predictive methods for void fraction

The literature includes five categories of void fraction prediction methods: (1) *homogeneous flow model*, (2) *slip ratio model*, (3) *drift flux model*, (4) *miscellaneous correlations/models* and (5) *numerical models*, each having its own application range. It is important to note that many of these models and correlations are based on experimental work involving adiabatic two-phase, two component flows (*e.g.*, air-water and air-oil). Overall, thermophysical property differences between two-component and one-component flows are significant, let alone the fact that the latter are highly influenced by wall heating. Therefore, relations based entirely on gas-liquid flow data may not be suitable for diabatic vapor-liquid flow and are, therefore, not discussed in the present paper. In this section, only widely used liquid-vapor void fraction relations, Table 3, will be introduced.

4.1. Homogeneous flow model

Combining the definitions of void fraction and vapor quality yields the following relation for one-dimensional (slip) two-phase flow:

$$\alpha = \frac{1}{1 + S\frac{1-x}{x}\frac{\rho_g}{\rho_f}} \tag{4}$$

For homogeneous flow, the liquid and vapor phases are assumed to possess the same velocity, *i.e.*, the slip ratio S ($= u_g/u_f$) equals unity. This reduces Eq. (4) for homogeneous flow to

$$\alpha_{\mathrm{H}} = \frac{1}{1 + \frac{1-x}{x}\frac{\rho_g}{\rho_f}} \tag{5}$$

Eq. (5) is by far the simplest equation for determining void fraction. As shown in Table 3, several relations are essentially variations to the homogeneous flow void fraction, α_{H}.

4.2. Slip ratio model

In general, the value of slip ratio S is greater than unity, especially for vertical upflow, where buoyancy tends to increase vapor velocity compared to that of liquid. The slip ratio models are based on the assumption that the two phases acquire their own uniform velocities and include an expression for S that generally depends on thermophysical properties and inlet conditions. As indicated in Table 3, some of slip flow relations are based on the Lockhart-Martinelli parameter, X_{tt}, which is square root of the ratio of liquid to vapor pressure gradients.

4.3. Drift flux model

Zuber and Findlay [74] were among the earliest investigators to propose general framework for the drift-flux model to determine void fraction according to the relation

$$\alpha = \frac{x}{C\left[x + \frac{\rho_g}{\rho_f}(1-x)\right] + \frac{\rho_g u_{gj}}{G}} \tag{6}$$

where C is termed 'distribution parameter' and u_{gj} 'drift velocity,' which take into account effects of non-uniform flow profile and local relative velocity between the phases, respectively. Differences among the various drift flux models lies in the choice of expressions for C and u_{gj}, which are different for different flow pattens, and obtained either empirically or theoretically.

4.4. Miscellaneous relations

Some void fraction relations do not belong to either of the above categories and are formulated empirically or semi-empirically based on data. Examples include the mechanistic model by Levy [75], which is based on the assumption of equal friction and head losses, and the correlation by Yamazaki and Yamaguchi [76], with include a parameter accounting for relative velocity between the two phases.

It is important to note that most of the void fraction relations in Table 3 are based on experimental investigations conducted within a limited range of operating conditions. Therefore, assumptions regarding their validity beyond original ranges warrant careful assessment.

4.5. Numerical models

Numerical models are generally multidimensional and more mechanistic than the above four categories of models and correlations. For example, Lai and Farouk constructed a 2D two-phase non-equilibrium model for the purpose of predicting void fraction distribution [77], which employs mass, momentum and energy conservations equations for each phase, along with a wall heat flux partitioning model and interfacial interaction relations for closure. Certain numerical models require implementing fundamental relations for bubble parameters, such as nucleation site density and bubble departure diameter and frequency [78–80], and bubble departure diameter appears to have stronger influence on predictions than nucleation site density [81]. And certain thermo-hydraulic codes [82] require implementing flow regime transition criteria is the sub-models used.

Table 3
Models and correlations for void fraction, α, applicable to subcooled flow boiling.

Author(s)	Formulae	Remarks
Modified homogenous model		
Armand & Treščev [83] (1959)	$\alpha = (0.833 + 0.167x)\alpha_H$	
Bankoff [84] (1960)	$\alpha = (0.71 + 0.0145p)\alpha_H$ or $\alpha = (0.71 + 0.0131p)\alpha_H$	p is in MPa, p = 0.49-20.62 MPa
Massena [85] (1960)	$\alpha = \begin{cases} 0.833\alpha_H & \alpha_H < 0.9 \\ (0.833 + 0.167x)\alpha_H & \alpha_H \geq 0.9 \end{cases}$	
Jones [86] (1961)**	$\alpha = [0.71 + 0.0131p + (0.29 - 0.0131p)\alpha^s]\alpha_H$	p is in MPa, $s = 3.53125 - 0.02719p + 0.01233p^2$
Nishino & Yamazaki [87] (1963)	$\alpha = 1 - (\frac{1-x}{x}\frac{\rho_g}{\rho_f}\alpha_H)^{0.5}$	
Chisholm [88] (1983)	$\alpha = \frac{\alpha_H}{\alpha_H + (1-\alpha_H)^{0.5}}$	
Löscher**	$\alpha = \alpha_H - \alpha_H^{1.39}(1-\alpha_H)^{0.8}(\frac{g\rho_f^2 D}{G^2})^{0.25}(1 - \frac{p}{p_c})^{3.4}(\frac{p}{p_c})^{-0.22}$	
Kütücüglu**	$\alpha = \alpha_H - (1-\alpha_H)^{0.5}(\frac{G^2}{g\rho_f^2 D})^{0.2}(1 - \frac{p}{p_c})^2$	
Kowalczewski**	$\alpha = \alpha_H - 0.71(1-\alpha_H)^{0.5}(\frac{g\rho_f^2 D}{G^2})^{0.045}(1 - \frac{p}{p_c})$	
Moussali**	$\alpha = [1 - \frac{30.4\frac{\rho_f}{\rho_g}\frac{x}{1-x}+11}{60(1+1.6\frac{\rho_f}{\rho_g}\frac{x}{1-x})(1+3.2\frac{\rho_f}{\rho_g}\frac{x}{1-x})}]\alpha_H$	
Slip ratio model		
Maurer [89] (1960)**	$\alpha = \frac{1}{1+(\frac{1-x}{x})^{0.6819+0.01217p}\exp(0.08951p-2.6439)}$ or $\alpha = \frac{1}{1+0.8(\frac{1-x}{x})^{0.6819+0.01217p}(\frac{\rho_g}{\rho_f})^{0.6}}$	p = 6.9-13.8 MPa
Fauske [90] (1961)	$\alpha = \frac{1}{1+\frac{1-x}{x}(\frac{\rho_g}{\rho_f})^{1/2}}$	p = 275.8-2482.1 kPa, D = 3.175-12.7 mm
Thom [91] (1964)	$\alpha = \frac{Ex}{1+x(E-1)}$, where E is a function of pressure p (bar) 1.014 17.24 41.38 86.21 144.83 206.9 221.1 E 246.0 40.0 20.0 9.8 4.95 2.15 1.0	$E = (\frac{\rho_f}{\rho_g})^{0.888}(\frac{\mu_g}{\mu_f})^{0.1776}$ [92]
Zivi [93] (1964)	$\alpha = \frac{1}{1+\frac{1-x}{x}(\frac{\rho_g}{\rho_f})^{2/3}}$	
Turner & Wallis [94] (1965)	$\alpha = \frac{1}{1+X_{tt}^{0.8}}$	$X_{tt} = (\frac{\mu_f}{\mu_g})^{0.1}(\frac{\rho_g}{\rho_f})^{0.5}(\frac{1-x}{x})^{0.9}$
Smith [95] (1967)	$\alpha = \{1 + 0.4\frac{\rho_g}{\rho_f}(\frac{1}{x} - 1) + 0.6\frac{\rho_g}{\rho_f}(\frac{1}{x} - 1)[\frac{\rho_f/\rho_g + 0.4(1/x-1)}{1+0.4(1/x-1)}]^{1/2}\}^{-1}$	
Wallis (1969) [96]#	$\alpha = (1 + X_{tt}^{0.8})^{-0.38}$	
Ahmad [49] (1970)	$\alpha = \frac{1}{1+\frac{1-x}{x}(\frac{G\mathrm{D}}{\mu_f})^{-0.016}(\frac{\rho_f}{\rho_g})^{-0.795}}$	
Chisholm [97] (1973)	$\alpha = \frac{1}{1+\frac{1-x}{x}\frac{\rho_g}{\rho_f}\sqrt{1-x(1-\frac{\rho_f}{\rho_g})}}$	
Madsen [98] (1975)	$\alpha = \frac{1}{1+(\frac{1-x}{x})^a(\frac{\rho_g}{\rho_f})^{-0.5}}$	$a = 1 + \log(\frac{\rho_f}{\rho_g})[\log(\frac{1-x}{x})]^{-1}$
Spedding & Chen [99] (1979)	$\alpha = \frac{1}{1+2.22(\frac{1-x}{x})^{0.65}(\frac{\rho_g}{\rho_f})^{0.65}}$	
Chen [100,101] (1981, 1986)	$\alpha = \frac{\varphi}{\varphi + X_{tt}^{2/3}}$	φ is a function of system pressure, tube diameter and liquid-vapor interfacial characteristics
Khalil *et al.* [102] (1981)	$\alpha = \frac{1}{1+(3+27.3x)\frac{1-x}{x}\frac{\rho_g}{\rho_f}}$	p = 1-2 atm, D = 6.35, 2.75 mm, Q = 5-35 L/h
Winterton [103](1981)	$\alpha = \frac{1}{1+[0.93(\frac{\rho_g}{\rho_f})^{0.11} + 0.07(\frac{\rho_g}{\rho_f})^{0.561}]\frac{1-x}{x}\frac{\rho_g}{\rho_f}}$	
Cioncolini & Thome [43] (2012)	$\alpha = \frac{m_1 x^{m_2}}{1+(m_1-1)x^{m_2}}$	$m_1 = 3.129(\rho_g/\rho_f)^{-0.2186} - 2.129$, $m_2 = 0.6513(\rho_g/\rho_f)^{0.5150} + 0.3487$
Drift-flux model		
Nicklin [104] (1962)	$C = 1.2$, $u_{gj} = 0.35\sqrt{gD}$	
Zuber & Findlay [74] (1965)	$C = 1.20$ and $u_{gj} = 1.18[g\sigma(\rho_f - \rho_g)/\rho_f^2]^{1/4}$	
GE-Ramp (1970)	If $\alpha \leq 0.65$, $C = 1.1$ and $u_{gj} = 2.9[g\sigma(\rho_f - \rho_g)/\rho_f^2]^{1/4}$. Otherwise, $C = 1$	
	+ $0.1(1 - \alpha)/0.335$ and $u_{gj} = 2.9(1-\alpha)[g\sigma(\rho_f - \rho_g)/\rho_f^2]^{1/4}/0.335$	
Rouhani & Axelsson [105] (1970)	$C = 1.12$ and $C = 1.54$ for low G, and $u_{gj} = 1.18[g\sigma(\rho_f - \rho_g)/\rho_f^2]^{1/4}$	
Rouhani & Axelsson ++	$C = 1.2 - 0.2x$ or $C = 1 + 0.2(1-x)(gD\rho_f^2/G^2)^{1/4}$,	
Dix [66] (1971)	$C = \frac{x\rho_f}{x\rho_f + (1-x)\rho_g}[1 + \frac{(1-x)\rho_g}{x\rho_f}]^b$, $b = (\rho_f/\rho_g)^{0.1}$, $u_{gj} = 2.9[g\sigma(\rho_f - \rho_g)/\rho_f^2]^{1/4}$	
Saha & Zuber [50] (1974)	$C = 1.13$ and $u_{gj} = 1.41[g\sigma(\rho_f - \rho_g)/\rho_f^2]^{1/4}$	
Nabizadeh (1977)+	$C = \alpha_H[1 + \frac{G^{0.2}}{\rho_f^{0.2}N}g^{-0.1}D^{-0.1}(\frac{\rho_g}{\rho_f})^N(\frac{1-x}{x})^{1.22N}]$, $u_{gj} = 1.18[g\sigma(\rho_f - \rho_g)/\rho_f^2]^{1/4}$	$N = \sqrt{0.6(\rho_f - \rho_g)/\rho_f}$
Ishii [106] (1977)*	For churn turbulent flow, $C = 1.2 - 0.2\sqrt{\rho_g/\rho_f}[1 - \exp(-18\alpha)]$, $u_{gj} = (C-1)j + \sqrt{2}(g\sigma\Delta\rho/\rho_f^2)^{1/4}$ For annular flow, $C = 1 + \frac{1+\alpha}{\alpha + \sqrt{\frac{\rho_g}{\rho_f}}[\frac{1+75(1-\alpha)}{\sqrt{\alpha}}]}$, $u_{gj} = (C-1)[j + \sqrt{\frac{gD\Delta\rho(1-\alpha)}{0.015\rho_f}}]$	
Ishii (1977)++	$C = \min(C_{11}, C_{12})$, where $C_{11} = 1.2 - 0.2\sqrt{\rho_g/\rho_f}[1 - \exp(-18\alpha)]$, $C_{12} = 1 + \frac{1-\alpha}{0.8+4\sqrt{\rho_g/\rho_f}}$ ++. $u_{gj} = \min(u_{gj1}, u_{gj2})$, where $u_{gj1} = 1.43[g\sigma(\rho_f - \rho_g)/\rho_f^2]^{1/4}$, $u_{gj2} = \frac{1-\alpha}{\alpha + [\frac{1+75(1-\alpha)}{\alpha^{1/2}}\frac{\rho_g}{\rho_f}]^{1/2}}\{j + [\frac{(\rho_f - \rho_g)gD(1-\alpha)}{0.015\rho_f}]^{1/2}\}$	
Ünal [107] (1977)	$C = 1.00$ and $u_{gj} = 0.36[1 - (p/p_c)]^{0.9}$	p = 2-15.9 MPa, D = 4.7-34.3 mm, G = 388-3500 kg/m^2.s, q" = 1-200 W/cm^2; various tube geometries.

(*continued on next page*)

Table 3 (*continued*)

Author(s)	Formulae	Remarks
Ünal [108] (1978)	$C=1.03$ and $u_{gj}=16.1[g\mu_f(\rho_f-\rho_g)/\rho_f^2]^{1/3}$	p=4.3-18 MPa, D=8 mm, G=51-107 kg/m^2.s, $\Delta T_{sub,out}$=0-1.3 K
Sun *et al.* [109] (1981)	$C=[0.82+0.18(p/p_c)]^{-1}$, $u_{gj}=1.41[g\sigma(\rho_f-\rho_g)/\rho_f^2]^{1/4}$ for saturated region, and $C=\frac{x\rho_f}{x\rho_f+(1-x)\rho_g}[1+\frac{(1-x)\rho_g}{x\rho_f}]^b$, $b=(\rho_f/\rho_g)^{0.1}$, $u_{gj}=1.18[g\sigma(\rho_f-\rho_g)/\rho_f^2]^{1/4}(1-x)$ for subcooled region	
Liao *et al.* (1985)*	For bubbly flow $j_f>2.34-1.07(g\sigma\Delta\rho/\rho_f^2)^{1/4}$, $C=1.00$ and $u_{gj}=1.53(1-\alpha)^2(g\sigma\Delta\rho/\rho_f^2)^{1/4}$. For churn turbulent flow, $C=1.2-0.2\sqrt{\rho_g/\rho_f}[1-\exp(-18\alpha)]$, $u_{gj}=0.33(g\sigma\Delta\rho/\rho_g^2)^{1/4}$. For annular flow, $j_g>(gD\Delta\rho/\rho_g)^{1/2}(1/C-0.1)$, $C=1+(1+\alpha)/(\alpha+4\sqrt{\rho_g/\rho_f})$, $u_{gj}=(C-1)\sqrt{\frac{gD\Delta\rho(1-\alpha)}{0.015\rho_f}}$	
Sonnenburg [110] (1989)	$C=1.32-0.32(\rho_g/\rho_f)^{0.5}$, $u_{gj}=\frac{C(1-C\alpha)\sqrt{gD(\rho_f-\rho_g)}}{\sqrt{gD(\rho_f-\rho_g)}+C\alpha\sqrt{\rho_g}-C\alpha\sqrt{\rho_f}}$	
Bestion [111] (1990)	$C=1.00$ and $u_{gj}=0.188[gD(\rho_f-\rho_g)/\rho_g]^{1/2}$	
Chexal *et al.* (1992)*	$C=\frac{1-\exp(-C_1\alpha)}{[1-\exp(-C_1)][K_0+(1-K_0)\alpha^r]}$, $u_{gj}=1.41(\frac{gD\Delta\rho}{\rho_f^2})^{1/4}C_2C_3C_4C_5$, where $r=\frac{1+1.57\rho_g/\rho_f}{1-K_1}$, $K_0=K_1+(1-K_1)(\rho_g/\rho_f)^{1/4}$, $K_1=\min[0.8,\frac{1}{1+\exp[-\max(\mathrm{Re}_f,\mathrm{Re}_g)/60000]}]$.	$C_1=\frac{4p_c^2}{p(p_c-p)}$, $C_2=$ $\begin{cases}0.4757[\ln(\frac{\rho_f}{\rho_g})]^{0.7}, \text{if}\rho_f/\rho_g<18\\1, \text{if}\rho_f/\rho_g<18\text{and}C_6\geq 1\\[1-\exp(\frac{-C_6}{1-C_6})]^{-1}, \text{if}\rho_f/\rho_g<18\text{and}C_6<1\end{cases}$ $C_3=\max[0.5, 2\exp(\frac{-\mathrm{Re}_f}{60000})]$ $C_4=$ $\begin{cases}1, \text{if}C_7\geq 1\\[1-\exp(\frac{-C_7}{1-C_7})]^{-1}, \text{if}C_7<1\end{cases}$, $C_5=(1-\alpha)^{K_1}$ $C_6=\sqrt{150\rho_g/\rho_f}$, and $C_7=(0.09144/D)^{0.6}$
Takeuchi *et al.* (1992)*	$C=1.11775$ + $0.45881\alpha-0.57656\alpha^2$, $u_{gj}=\frac{C(1-C\alpha)Dg\Delta\rho}{1.367^2+C\alpha(\sqrt{\rho_g/\rho_f}-1.367^2)}\sqrt{\frac{D}{\sigma\rho_f}}\min(\frac{1}{2.4},\frac{10.24}{D}\sqrt{\frac{\sigma}{g\Delta\rho}})$	
Miscellaneous correlations/models		
Levy [75] (1960)	$x=\frac{\alpha(1-2\alpha)+\alpha(1-\alpha)\sqrt{1-2\alpha+2\alpha\rho_f/\rho_g}}{2\rho_f(1-\alpha)^2/\rho_g+\alpha(1-2\alpha)}$	
Yamazaki & Yamaguchi [76] (1976)	$\frac{\alpha}{(1-\alpha)(1-K\alpha)}=\frac{\rho_f}{\rho_g}\frac{x}{1-x}$	$K=\begin{cases}1 & K'\geq 2\times10^{-6}\\0.57 & K'<2\times10^{-6}\end{cases}$, $K'=\frac{(\rho_f-\rho_g)gD\mu_f^2}{\rho_f\sigma^2}$
Gardner [112] (1980)	$\frac{\alpha}{\sqrt{1-\alpha}}=a_1[\frac{\sqrt{\rho_f}xG}{(\Delta\rho g\sigma)^{1/4}\rho_g}]^{2/3}[\frac{\rho_g v_f^2\sqrt{\Delta\rho g}}{\sigma^{3/2}}]^{2a_2/3}$	p=0.127-19 MPa.
Tandon *et al.* (1985) [113]	$\alpha=\begin{cases}1-\frac{1.928\mathrm{Re}_f^{-0.315}}{F(X_{tt})}+\frac{0.9293\mathrm{Re}_f^{-0.63}}{[F(X_{tt})]^2}, 50<\mathrm{Re}_f<1125\\1-\frac{0.38\mathrm{Re}_f^{-0.088}}{F(X_{tt})}+\frac{0.0361\mathrm{Re}_f^{-0.176}}{[F(X_{tt})]^2}, \mathrm{Re}_f>1125\end{cases}$	$F(X_{tt})=0.15(X_{tt}^{-1}+2.85X_{tt}^{-0.476})$
Huq & Loth [114] (1992)	$\alpha=1-\frac{2(1-x)^2}{1-2x+[1+4x(1-x)(\rho_f/\rho_g-1)]^{1/2}}$	

* From ref. [42]
** From ref. [115]
\# From ref. [41]##From ref. [32]
\+ From ref. [116]
++ From ref. [34]

In the remainder of this paper, numerical models will be addressed only briefly for completeness, but excluded from further assessment against available experimental data.

5. Consolidated database

To evaluate the predictive tools discussed in the previous sections, a consolidated database for subcooled vertical upflow boiling in a circular tube is amassed from prior works. It includes 61 $x_e|_{NVG}$ data points from 5 sources, which are summarized in Table 4, and 1118 void fraction data points from 11 sources, Table 5. The data are obtained either directly from the original sources or extracted from digitalized figures using commercial software.

The ranges of operating conditions for the consolidated database are as follows:

1. $x_e|_{NVG}$ data:
   - Fluid: water
   - Inlet pressure: p_{in} = 0.1-15 MPa
   - Tube diameter: D = 11.3-24.0 mm
   - Heat flux: q'' = 1.45-221 W/cm^2
   - Mass velocity: G = 27.5-3438 kg/m^2.s

Table 4
Experimental studies on subcooled vertical upflow boiling in a circular tube used to obtain $x_e|_{NVG}$ data.

Author(s)	D (mm)	p_{in} (MPa)	G (kg/m^2.s)	q'' (W/cm^2)	n
Ferrell [117] (1964)*	11.8	0.41-1.65	529-1318	24-68	11
Bartolomei & Chanturiya [118] (1967)**	15.4, 24.0	1.5-4.5	900	38-80	11
Edelman & Elias [119] (1981)	11.3	0.10	27.5-185	1.45-9.55	16
Bartolemei *et al.* [120] (1982)**	12	3-15	405-2123	42-221	20
Labuntsov *et al.* [121] (1984)**	12.1	2-7	794-3438	58-116	3
Overall	11.3-24.0	0.10-15	27.5-3438	1.45-221	61

* From ref. [59]
** From ref. [61]

Table 5
Experimental studies on subcooled vertical upflow boiling in a circular tube used to obtain void fraction, α, data.

Author(s)	Liquid	D (mm)	p_{in} (MPa)	$\Delta T_{sub,in}$ (K)	G (kg/m^2.s)	q" (W/cm^2)	n^+
Rouhani & Becker [122] (1963)	heavy water	6.10	0.67-5.96	NI	661-2030	36.5-130.4	149 (149)
Ferrell [117] (1964)	water	11.8364	0.41-1.65	27-126	487-1785	24-68	679 (365)
Bartolomei & Chanturiya [118] (1967)*	water	24.0	1.5-4.5	23-54	888	38-78	76 (72)
Thom *et al.* [123] (1967)	water	9.7536	5.2-6.9	40.6-65.8	690-953	46.8-90.5	23 (23)
Kroeger & Zuber [47] (1968)	R22	10.1	1.15-3.25	13-25	131-487	1.4-4.2	18 (15)
Fung & Groeneveld [124] (1980)	water	11.94	0.1	5.1-20	495	18.2-28.1	20 (15)
Dimmick & Selander [125] (1990)**	water	12.29	0.165	27.5-61	620-1115	47.2-116.4	103 (47)
Bartolomey#	water	12.03	3-15	14-141	405-2123	42-221	368 (294)
Labuntsov#	water	12.1	7	33-67.5	730-2960	61.8-120	8 (6)
Rouhani#	water	10	0.96-5	80.6-170.7	126-130	58.9-91.9	65 (64)
Sabotinov#	water	11.7	6.79-6.86	18.5-97	419-1000	43-168.8	82 (68)
Overall	water, R22	6.10-24.0	0.1-15	5-170.7	126-2960	1.4-168.8	1591 (1118)

$^+$ Numbers in brackets indicate data point numbers actually used, which exclude data upstream the NVG point
* From ref. [126]
** From ref. [79]
# From ref. [127]

2. Void fraction data:
   - Fluids: water, R22
   - Inlet pressure: $p_{in} = 0.1$-15 MPa
   - Inlet subcooling: $\Delta T_{sub,in} = 5$-170.7 K
   - Tube diameter: $D = 6.1$-24.0 mm
   - Heat flux: $q" = 1.4$-168.8 W/cm^2
   - Mass velocity: $G = 126$-2960 kg/m^2.s

6. Assessment of models and correlations

When comparing the consolidated database to predictions of the previous models or correlations, all thermophysical properties of the working fluids are obtained from NIST's REFPROP 8.0 software [128]. As indicated in the previous sections, calculation of void fraction requires knowledge of local quality, x, which in turn is a function of both $x_e|_{NVG}$ and x_e. The procedure for calculating void fraction is as follows.

(1) Input the inlet condition parameters, such as p_{in}, D, G, $\Delta T_{sub,in}$ and q'', and then calculate the axial distribution of thermodynamic equilibrium quality, x_e, using Eq. (2).
(2) Calculate thermodynamic equilibrium quality at the net vapor generation point, $x_e|_{NVG}$, using the different relations from Table 1. If the calculated $x_e|_{NVG}$ is less than $x_{e,in}$, $x_e|_{NVG}$ is substituted by the value of $x_{e,in}$. Otherwise, proceed to Step (3).
(3) Calculate the axial distribution of vapor quality, x, using the relations from Table 2.
(4) Calculate the axial distribution of void fraction, α, using the relations from Table 3.

In the subsequent sections, the different methods for calculating $x_e|_{NVG}$, x, and α will be first assessed, and a new and rather simple correlation for α with superior predictive accuracy is proposed.

6.1. Calculation of thermodynamic equilibrium quality at the point of net vapor generation, $x_e|_{NVG}$

As discussed in the previous section, accurate knowledge of thermodynamic equilibrium quality at the NVG point, $x_e|_{NVG}$, is an important prerequisite for void fraction calculation. In the present study, mean absolute error (MAE) is used to assess the accuracy and reliability of the relations listed in Table 1, and is defined as

$$\mathrm{MAE} = \frac{1}{n}\sum_i \frac{\left|\chi_{i,\mathrm{pred}} - \chi_{i,\mathrm{exp}}\right|}{\chi_{i,\mathrm{exp}}} \times 100\% \qquad (7)$$

where $\chi_{i,\mathrm{pred}}$ and $\chi_{i,\mathrm{exp}}$ are, respectively, predicted and measured values. In this section, χ indicates $x_e|_{NVG}$.

The MAE calculations reveal that, despite being one of the earliest tools for predicting $x_e|_{NVG}$, Saha and Zuber's correlation shows the highest accuracy (MAE = 20.31%) of all relations from Table 1, followed by Ha *et al.*'s correlation (MAE of 21.60%). Fig. 2 compares $x_e|_{NVG}$ values from the consolidated database with predictions of the four best performing relations. All other relations are found to show significant predictive errors, Table 6, presumably because of being assessed beyond their original validity ranges.

It needs to be mentioned that the relations by Ahmad [49] and Siman-Tov *et. al.* [70] are not included in the assessment study since they both require knowledge of inlet liquid subcooling, information not available from a vast majority of data sources. The relation by Kataoka *et. al.* [71] is also excluded because it modifies the Saha and Zuber's correlation [50] using the multiplier $q''/8800$, where q'' is in kW/m^2. Using the experimental data from Table 4, the value of this multiplier is smaller than 0.2, rendering this relation far less accurate than Saha and Zuber's. After comprehensive consideration, the popular Saha and Zuber correlation is recommended for prediction of $x_e|_{NVG}$.

6.2. Calculation of vapor quality, x

Referring back to Table 2, three different methods are available for calculating vapor quality in subcooled boiling. However, two of those, Bowring (Method 1) and Sekoguchi *et al.*, are excluded from consideration for ultimate calculation of void fraction because both are dependent on their own relations for $x_{e,NVG}$, which have been shown earlier to be far less accurate than Saha and Zuber's $x_{e,NVG}$ correlation. Furthermore, both methods show unrealistic predictions of vapor quality. This shortcoming is captured in Table 7 for four different sets of operating conditions, where both methods show physically unacceptable values of vapor quality in excess of unity, especially for cases with $x_e = 0.8$. Note also that the method of Sekoguchi requires iteration, which itself depends on the vapor quality calculation.

Of the three void fraction calculation methods, only the one by Saha and Zuber [50] is shown to yield physically acceptable values across broad ranges of conditions. Furthermore, it correctly predicts that, as x_e tends to unity, x also asymptotically approaches unity. The Saha and Zuber correlation also satisfied two important limits: (1) $x = 0$ at the NVG point, where $x_e = x_e|_{NVG}$ and the vapor generation is negligible, and (2) $x \to x_e$ in the saturated boiling region, where $x_e \gg x_e|_{NVG}$,. Because of these facts, only Saha and Zuber's method is selected for ultimate calculation of the void fraction.

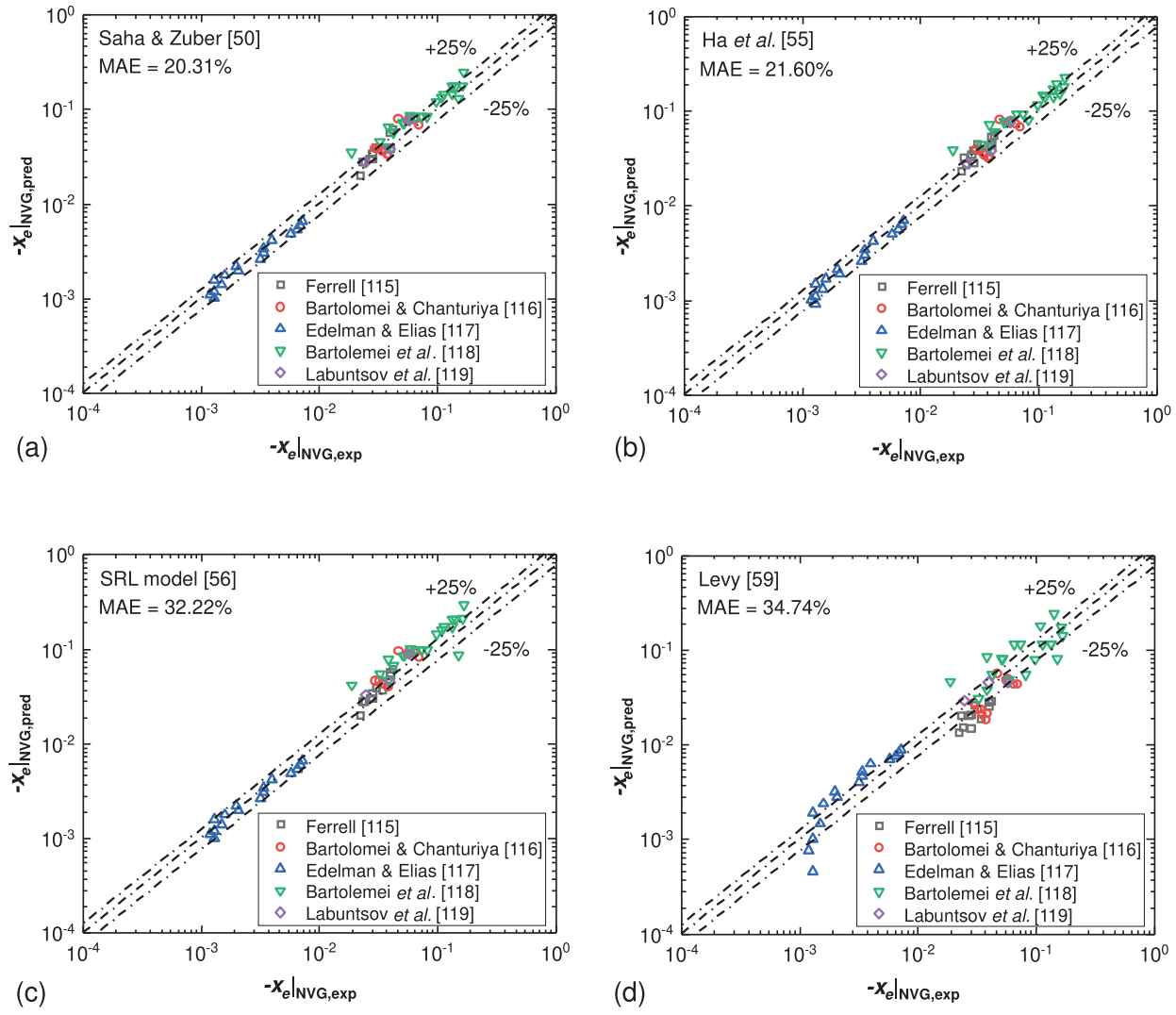

Fig. 2. Comparison of $x_e|_{NVG}$ values from the consolidated database with predictions of the four best performing tools: (a) Saha and Zuber correlation, (b) Ha *et al.* correlation, (c) SRL model, and (d) Levy model.

Table 6
Mean absolute errors of 13 $x_e|_{NVG}$ predictive methods against experimental data.

Author(s)	Overall MAE	Ferrell [117]	Bartolomei & Chanturiya [118]	Edelman & Elias [119]	Bartolemei *et al.* [120]	Labuntsov *et al.* [121]
Griffith *et al.* (1958)	155.52	45.62	47.29	491.43	23.77	42.19
Levy (1967)	34.74	32.99	29.11	34.44	41.61	17.49
Dix (1971)	159.78	40.73	125.15	128.75	262.28	205.53
Saha & Zuber (1974)	20.31	17.36	23.02	11.87	27.97	15.16
Ünal (1975)	73.01	24.43	23.96	219.51	17.79	17.78
Sekoguchi *et al.* (1980)	717.30	118.51	69.52	2525.07	53.66	71.02
Kalitvianski (2000)	193.62	291.04	82.61	367.73	82.76	53.80
Sun *et al.* (2003)	68.67	23.74	24.86	184.31	32.35	19.42
Ha *et al.* (2005)	21.60	19.53	22.32	12.20	30.96	14.32
Ha *et al.* (2018)	93.31	31.73	44.74	240.89	42.80	46.89
Ha *et al.* (2019)	41.51	18.25	21.13	87.47	32.49	16.52
Ha *et al.* (2020)	50.80	29.61	25.50	87.47	49.34	35.40
SRL Model	32.22	19.58	39.47	11.87	51.59	31.35

Table 7
Comparison of calculated values of vapor quality, x, using different relations for $p_{in} = 100$ kPa, $\Delta T_{sub,in} = 20$ K, $D = 10$ mm and $q'' = 15$ W/cm^2.

Cases	G	x_e	$x_e\|_{NVG}$			x		
	kg/m^2.s		Saha & Zuber	Sekoguchi	Bowring	Saha & Zuber	Sekoguchi	Bowring
1.1	800	0.800	-0.009	-0.030	-0.005	0.800	1.509	0.854
1.2	800	0.020	-0.009	-0.030	-0.005	0.020	0.020	0.003
2.1	1250	0.800	-0.008	-0.022	-0.003	0.800	1.715	1.183
2.2	1250	0.020	-0.008	-0.022	-0.003	0.020	0.021	0.003

Table 8
Preliminary check of void fraction, α, relations corresponding to three limiting conditions.

Author(s)	Zero quality limit	Unity quality limit	Critical pressure limit
Homogeneous and modified models			
Homogeneous model	yes	yes	yes
Armand & Treščev (1959)	yes	yes	yes
Bankoff (1960)	yes	yes	yes
Massena (1960)	yes	yes	yes
Jones (1961)	yes	yes	yes
Nishino & Yamazaki (1963)	yes	yes	no
Chisholm (1983)	yes	yes	no
Löscher	yes	yes	yes
Kütücüglu	no	yes	yes
Kowalczewski	no	yes	yes
Moussali	yes	yes	no
Slip ratio model			
Maurer (1960)	yes	yes	no
Fauske (1961)	yes	yes	yes
Thom (1964)	yes	yes	yes
Zivi (1964)	yes	yes	yes
Turner & Wallis (1965)	yes	yes	no
Smith (1967)	yes	yes	yes
Wallis (1969)	yes	yes	no
Ahmad (1970)	yes	yes	no
Chisholm (1973)	yes	yes	yes
Madsen (1975)	yes ($x\rightarrow0$)	yes ($x\rightarrow1$)	yes
Spedding & Chen (1979)	yes	yes	no
Chen (1981, 1986)	yes	yes	no
Khalil *et al.* (1981)	yes	yes	no
Winterton (1981)	yes	yes	yes
Cioncolini & Thome (2012)	yes	yes	yes
All the drift-flux model			
	yes	no	no
Miscellaneous empirical correlations			
Levy (1960)	yes	yes	yes
Yamazaki & Yamaguchi (1976)	yes ($x\rightarrow0$)	yes ($x\rightarrow1$)	no
Gardner (1980)	yes	no	no
Tandon *et al.* (1985)	no	yes ($x\rightarrow1$)	no
Huq & Loth (1992)	yes	yes ($x\rightarrow1$)	yes

6.3. Calculation of void fraction, α

6.3.1. Preliminary check of relations

In this section, all the void fraction relations from Table 3 are initially checked for three important limiting conditions: (1) *zero quality limit* of $\alpha=0$ at $x=0$, (2) *unity quality limit* of $\alpha=1$ at $x=1$, and (3) *critical pressure limit* of $\alpha=x$ at $p=p_c$. As shown in Table 8, only 16 relations among a total of 49 asymptotically satisfy all three limiting conditions, and the remaining 33 relations fail to satisfy at least one of the limiting conditions. It is interesting to note that the popular drift-flux model fails to satisfy the unity quality limit unless $C+\rho_g u_{gj}/G=1$, and the critical pressure limit can be met only when $C=1$. But a simple inspection of the drift-flux relations from Table 3 shows that the values of C and u_{gj} seldom satisfy these two limiting conditions.

It is worth noting that many prior investigators attempted to correlate void fraction, α, with vapor quality, x, in pursuit of best overall predictions rather than simply meeting the limiting conditions. Therefore, the 33 relations failing to satisfy at least one of the limiting conditions are not excluded from further comparison with the consolidated database. Nonetheless, some of the same relations suffer the additional drawback of exhibiting erroneous predictions in some cases. For example, the correlation by Tandon *et al.* [113] predicts α values well above unity for even very small vapor quality conditions. Errors are exhibited by other relations as well, therefore any unrealistic values for α are excluded from comparison with the consolidated database.

6.3.2. Drift-flux model parameters

As can be seen in Table 3, a variety of expressions for distribution parameter, C, and drift velocity, u_{gj}, have been adopted by different investigators when employing the drift-flux model. Chexal *et al.* [129] proposed several limiting conditions for C and u_{gj}: (1) critical pressure limit ($p=p_c$), where the two phases become indistinguishable in both properties and velocity, therefore, C and u_{gj} should tend to 1 and 0, respectively, (2) zero pressure limit ($p\rightarrow0$), where $\rho_g/\rho_f\rightarrow0$, resulting in $C=1$ and $u_{gj}\rightarrow\infty$, (3) unity void

Table 9
Evaluation of drift-flux model parameters at four limiting conditions.

Models		Critical pressure limit		Zero pressure limit		Unity void fraction limit		Zero void fraction limit	
		C	u_{gj}	C	u_{gj}	C	u_{gj}	C	u_{gj}
Nicklin (1962)		no	no	no	no	no	no	no	yes
Zuber & Findlay (1965)		no	yes	no	no	no	no	no	yes
GE-Ramp (1970)		no	yes	no	no	no	no	no	yes
		no	yes	yes	no	yes	yes	no	yes
Rouhani & Axelsson (1970)		no	yes	no	no	no	no	no	yes
Dix (1971)		yes	yes	yes	no	yes	no	no	yes
Saha & Zuber (1974)		no	yes	no	no	no	no	no	yes
Nabizadeh (1977)		no	yes	yes	no	yes	no	no	yes
Ishii (1977)*		no	no	no	no	no	no	no	yes
		no	no	no	no	no	no	no	yes
Ishii (1977)++	C_{11}	no	–	no	–	no	–	no	–
	C_{12}	no	–	yes	–	yes	–	no	–
	u_{gj1}	–	yes	–	no	–	no	–	yes
	u_{gj2}	–	no	–	no	–	yes	–	yes
Ünal (1977)		yes	yes	yes	no	yes	no	no	yes
Ünal (1978)		no	yes	no	no	no	no	no	yes
Sun *et al.* (1981)		yes	yes	no	no	no	no	no	yes
		yes	yes	yes	no	yes	yes	no	yes
Liao *et al.* (1985)		yes	yes	yes	no	yes	yes	no	yes
		no	yes	no	no	no	no	no	yes
		no	yes	no	no	no	yes	no	yes
Sonnenburg (1989)		yes	no	no	no	no	no	no	yes
Bestion [71] (1990)		yes	yes	yes	no	yes	no	no	yes
Takeuchi *et al.* (1992)		no	no	yes	no	yes	yes	no	yes
Rouhani & Axelsson		no	–	yes	–	yes	–	no	–

* From ref. [42]
++ From ref. [34]

Table 10
Comparison of predictions of void fraction, α, models and correlations with the data.

Data/ Relations	Overall MAE	Rouhani & Becker [122] (1963)	Ferrell [117] (1964)	Bartolomei & Chanturiya [118] (1967)	Thom *et al.* [123] (1967)	Kroeger & Zuber [47] (1968)
Modified homogeneous model						
Homogeneous model	53.11	21.32	42.16	96.65	60.13	57.31
Armand & Treščev (1959)	36.26	5.94	29.11	68.69	40.88	46.17
Bankoff-1 (1960)	33.81	9.79	29.11	55.38	39.59	41.66
Bankoff-2 (1960)	33.49	10.00	29.12	54.70	39.11	41.75
Massena (1960)	35.86	5.49	29.02	68.28	41.37	45.55
Jones (1961)	33.41	6.29	24.53	59.06	35.85	45.53
Nishino & Yamazaki (1963)	29.00	16.31	21.00	34.13	28.95	44.02
Chisholm (1983)	36.54	5.66	28.10	73.01	48.25	47.88
Löscher	31.86	12.03	18.69	50.47	45.78	36.42
Kütücüglu	57.78	51.30	75.38	55.11	59.68	32.39
Kowalczewski	30.86	19.70	32.77	39.66	37.42	32.32
Moussali	46.36	18.00	38.05	82.45	47.28	51.69
Slip ratio model						
Maurer-1 (1960)	37.02	9.95	27.38	70.77	53.37	153.04
Maurer-2 (1960)	33.34	5.03	24.90	75.55	44.92	61.06
Fauske (1961)	53.44	45.14	56.68	60.24	46.00	44.33
Thom (1964)	25.79	7.04	17.31	38.36	21.29	41.26
Zivi (1964)	33.85	22.99	33.04	34.40	28.08	37.00
Turner & Wallis (1965)	39.46	38.57	46.98	29.58	39.12	42.69
Smith (1967)	34.69	4.74	25.99	68.82	45.13	47.32
Wallis (1969)	130.93	14.32	50.22	295.50	157.56	212.49
Ahmad (1970)	27.42	6.55	17.95	45.11	25.94	39.03
Chisholm (1973)	36.82	5.27	27.93	73.58	48.02	48.03
Spedding & Chen (1979)	30.76	18.38	23.04	51.17	45.00	51.02
Khalil *et al.* (1981)	36.80	32.45	21.21	32.01	43.43	61.89
Winterton (1981)	81.51	34.23	65.81	157.14	99.58	76.68
Cioncolini & Thome (2012)	93.74	13.58	59.41	245.80	122.15	119.36
Drift flux model						
Nicklin (1962)	32.43	5.85	28.30	58.78	36.94	33.53
Zuber & Findlay (1965)	31.49	5.74	27.57	59.23	35.60	32.82
Rouhani & Axelsson (1970)	34.62	7.51	29.04	67.51	38.38	32.44
Dix (1971)	26.32	6.63	20.67	44.65	17.45	35.02
Saha & Zuber (1974)	33.18	6.74	28.14	64.60	36.80	31.06
Nabizadeh (1977)	31.53	25.59	25.43	29.38	30.41	39.68
Ünal (1977)	38.32	15.57	32.27	71.96	39.91	26.26
Ünal (1978)	40.34	14.74	33.57	77.29	43.12	29.00
Bestion (1990)	30.93	14.88	22.60	52.80	38.77	24.56
Miscellaneous correlations/models						
Levy (1960)	30.92	22.70	33.95	24.62	31.93	38.85
Yamazaki & Yamaguchi (1976)	36.38	8.21	30.42	61.75	44.68	47.34
Tandon *et al.* (1985)	47.96	11.99	20.68	81.37	55.11	68.86
Huq & Loth (1992)	34.17	5.17	25.02	65.01	43.68	45.86
Present correlation						
	25.59	7.42	17.38	37.46	21.37	39.62
Average		14.97	31.75	70.30	46.45	52.07

Data Relations	Fung & Groeneveld [124] (1980)	Dimmick & Selander [125] (1990)	Bartolomey	Labuntsov	Rouhani	Sabotinov
Modified homogeneous model						
Homogeneous model	29.21	116.10	53.29	49.34	110.55	39.39
Armand & Treščev (1959)	20.26	91.06	37.71	44.67	78.39	21.95
Bankoff-1 (1960)	26.70	74.14	36.61	44.27	60.81	20.38
Bankoff-2 (1960)	26.71	74.10	35.73	44.14	59.87	20.10
Massena (1960)	20.25	91.03	37.18	44.56	76.48	21.35
Jones (1961)	22.71	79.64	36.90	44.19	78.51	21.69
Nishino & Yamazaki (1963)	21.47	59.72	36.34	48.33	42.05	25.75
Chisholm (1983)	18.91	92.40	39.60	44.81	72.67	21.68
Löscher	34.46	71.10	45.37	44.97	35.67	29.86
Kütücüglu	27.49	70.03	55.25	–*	26.70	40.64
Kowalczewski	11.98	26.26	36.41	–*	18.65	53.47
Moussali	28.48	105.38	44.66	46.98	103.44	33.47
Slip ratio model						
Maurer-1 (1960)	59.22	60.33	40.38	52.34	60.47	22.33
Maurer-2 (1960)	18.49	80.99	35.08	42.95	66.24	16.93
Fauske (1961)	68.52	88.65	55.65	74.88	18.01	45.84
Thom (1964)	21.43	49.25	32.28	47.69	60.79	18.99
Zivi (1964)	40.72	67.11	37.64	59.25	26.00	26.95
Turner & Wallis (1965)	61.58	69.25	33.18	34.24	19.69	31.69

(*continued on next page*)

Table 10 (*continued*)

Data/ Relations	Overall MAE	Rouhani & Becker [122] (1963)	Ferrell [117] (1964)	Bartolomei & Chanturiya [118] (1967)	Thom *et al.* [123] (1967)	Kroeger & Zuber [47] (1968)
Smith (1967)	18.90	87.92	38.29	43.76	71.99	19.80
Wallis (1969)	23.64	103.49	264.60	307.37	103.22	93.69
Ahmad (1970)	21.32	50.30	33.73	44.48	68.05	21.63
Chisholm (1973)	18.87	92.44	40.45	45.05	74.79	21.85
Spedding & Chen (1979)	22.44	67.46	33.82	38.98	40.16	22.16
Khalil *et al.* (1981)	19.95	53.51	54.98	64.71	27.32	47.41
Winterton (1981)	33.30	196.28	81.85	76.86	138.71	60.69
Cioncolini & Thome (2012)	14.51	167.08	130.88	175.95	105.97	64.90
Drift flux model						
Nicklin (1962)	20.74	86.52	34.80	44.27	50.54	20.10
Zuber & Findlay (1965)	20.92	84.45	34.46	44.22	41.78	20.01
Rouhani & Axelsson (1970)	19.77	91.85	38.11	44.97	49.72	21.82
Dix (1971)	21.15	59.15	36.34	58.13	16.86	22.60
Saha & Zuber (1974)	19.65	89.47	36.99	44.79	43.37	21.10
Nabizadeh (1977)	27.63	46.79	40.25	58.25	31.52	28.39
Ünal (1977)	24.14	97.10	43.49	45.86	37.50	27.48
Ünal (1978)	23.42	99.95	43.59	45.86	56.32	28.23
Bestion (1990)	27.97	61.00	41.84	45.71	21.83	26.30
Miscellaneous correlation/model						
Levy (1960)	50.75	59.46	29.43	36.73	29.43	20.52
Yamazaki & Yamaguchi (1976)	19.28	84.00	37.00	42.17	86.32	18.67
Tandon *et al.* (1985)	27.84	49.40	88.16	68.22	60.49	46.80
Huq & Loth (1992)	19.19	84.16	39.58	44.27	69.43	19.65
Present correlation						
	22.87	48.12	31.88	47.34	59.79	18.91
Average	26.92	80.66	49.59	58.83	57.50	30.13

* Negative void fraction values

fraction limit ($\alpha \to 1$), corresponding to pure vapor flow, where $C=1$ and $u_{gj}=0$, and (4) zero void fraction limit ($\alpha=0$), where $C=0$ and $u_{gj} > 0$. These same four criteria are employed in this section to evaluate the drift-flux models provided in Table 3. Table 9 shows that none of the 18 drift-flux models from Table 3 do satisfy all four limiting conditions, though they may provide acceptable results for intermediate operating conditions.

6.3.3. Vapor void fraction comparisons

It must be reiterated that the vast majority of void fraction relations are empirical or semi-empirical and based on experimental data obtained under various ranges of operating conditions. Given the strong influences of inlet pressure and mass velocity on bubble dynamics, those influences are reflected in several of the previous void fraction relations.

In this section, MAE is used to assess the predictive accuracy of individual void fraction relations. A few relations are excluded from consideration. They include those by Chen [100,101] and Gardner [112], because values of empirical constants in these relations depend on the specific sources of the data (operating conditions and liquid-vapor interfacial characteristics), with different values used for the different data sources.

Also excluded is the relation by Madsen [98], which incorrectly predicts α values much smaller than unity for the entire range of $0 \le x \le 1$. Also excluded are drift-flux models by GE-Ramp, Ishii [106], Liao *et al.*, Sonnenburg [110], Chexal *et al.* and Takeuchi *et al.* (from ref. [32]), which rely on drift flux parameters that are themselves functions of void fraction, therefore requiring complex iterative calculations to arrive at a void fraction prediction. It must also be noted that, although MAE values are provided for all remaining relations, some are not suitable for all operating conditions. For example, the relation by Tandon *et. al.* [113] yields infinite α value just downstream of the NVG point, and by Kütücüglu, Löscher and Kowalczewski (all three relations from ref. [115]) yield negative α values for low values of x.

Table 10 provides detailed MAE values for 40 void fraction relations against data from several individual sources, as well as those for a new correlation recommended by the present authors, which is discussed below. Most notable among the previous relations in terms of superior predictive accuracy are the slip ratio model by Thom [91], drift-flux model by Dix [66], slip ratio model by Ahmad [49], and modified homogeneous model by Nishino and Yamazaki [87], with MAE values of 25.79%, 26.32%, 27.42% and 29.00%, respectively. Fig. 3 shows comparisons of data with predictions for the same four relations, along with those of other popular relations by Levy [75], Saha and Zuber [50], Zivi [93], Smith [95], Yamazaki and Yamaguchi [76] and the homogenous model, in addition to the authors' newly proposed correlation. Notice when comparing the top preforming previous relations by Thom and Dix that, while the former shows the lowest MAE, the latter appears to provide less scatter. Also notable is that the Levy and Zivi relations generally underestimate the consolidated void fraction database, while those by Saha and Zuber, Smith, Yamazaki and Yamaguchi, and one according to the homogenous model overestimate.

6.3.4. Proposed new correlation

In this section, an attempt is made to develop a new correlation for void fraction which spans the broad overall ranges of operating conditions of the entire consolidate database.

As indicated by Butterworth [92], many prior dissimilar void fraction relations seem to adopt the common functional form

$$\alpha = \frac{1}{1 + s_1\left(\frac{1-x}{x}\right)^{s_2}\left(\frac{\rho_g}{\rho_f}\right)^{s_3}\left(\frac{\mu_g}{\mu_f}\right)^{s_4}} \tag{8}$$

Notice that values of two of the constants in this equation, s_1 and s_2, can be determined from the limiting condition of $\alpha = x$ at the critical pressure, where $\rho_g = \rho_f$ and $\mu_g = \mu_f$. This condition yields $s_1 = s_2 = 1$. Using a regression technique, values of the two remaining constants are determined as $s_3 = 0.8599$ and

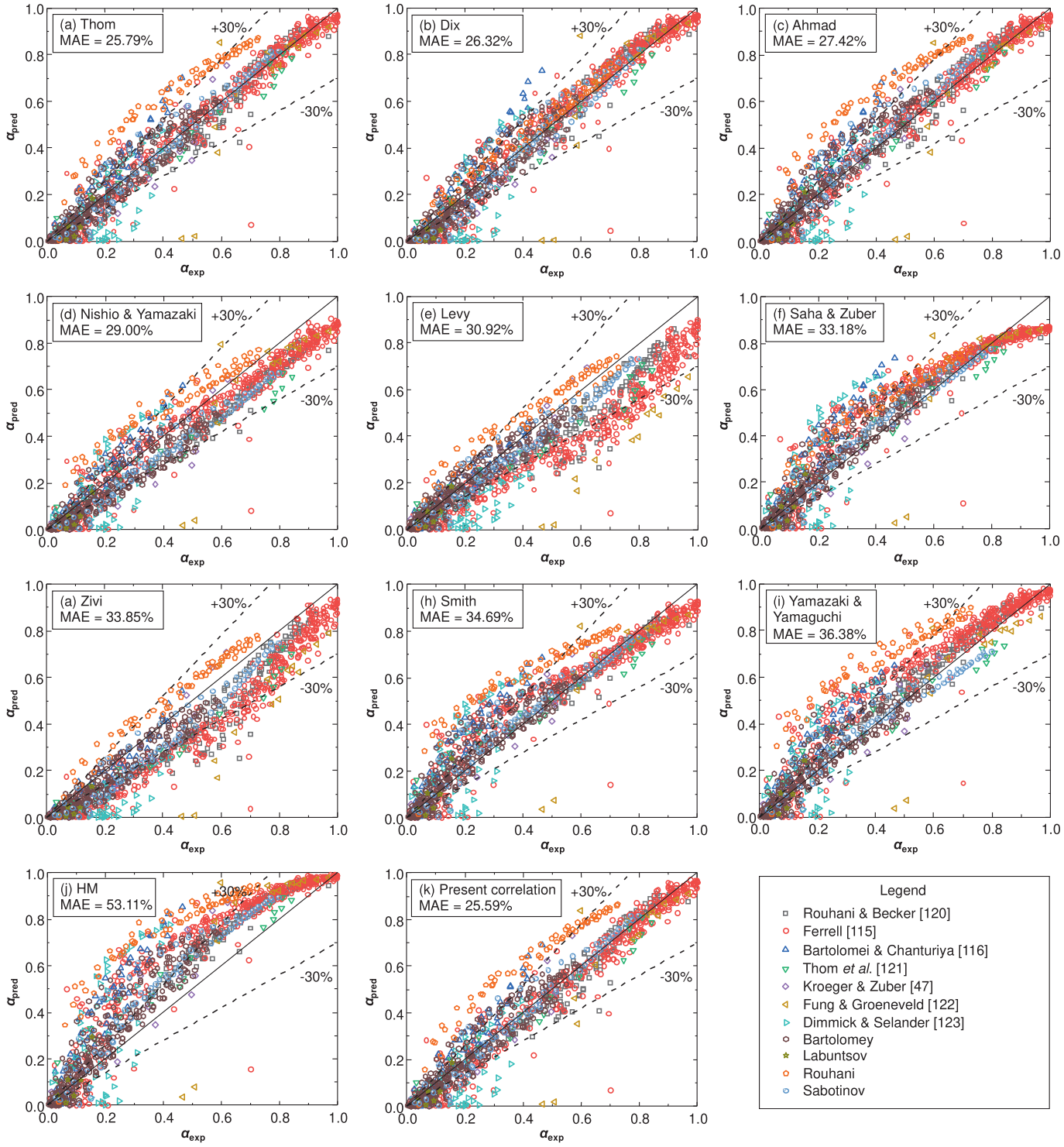

Fig. 3. Comparison of consolidated void fraction data with predictions according to relations by (a) Thom, (b) Dix, (c) Ahmad, and (d) Nishino and Yamazaki, (e) Levy, (f) Saha and Zuber, (g) Zivi, (h) Smith, (i) Yamazaki and Yamaguchi, and (j) homogenous model, along with (k) new relation proposed by the present authors.

$s_4 = -0.1448$. Since it is well known that void fraction is generally strongly influenced by both flow quality and density ratio and to a far lesser extent viscosity ratio [39], Eq. (8) can be simplified further by eliminating the viscosity ratio term and re-employing the regression technique, which yields the final form for the authors' newly proposed relation.

$$\alpha = \frac{1}{1 + \frac{1-x}{x}\left(\frac{\rho_g}{\rho_f}\right)^{0.7988}} \tag{9}$$

Notice from Table 10 and Fig. 3 that, despite its very simple form, the new relation has a MAE of 25.59%, slightly better than Thom's, the best performing prior correlation.

6.3.5. Segregation of predictions according to lower versus higher ranges of void fraction

Some of the large MAE values for void fraction in Table 10 can be attributed to a number of factors. First, correlations are generally based on a limited range of experimental operating conditions, which renders extrapolations beyond their validity range un-

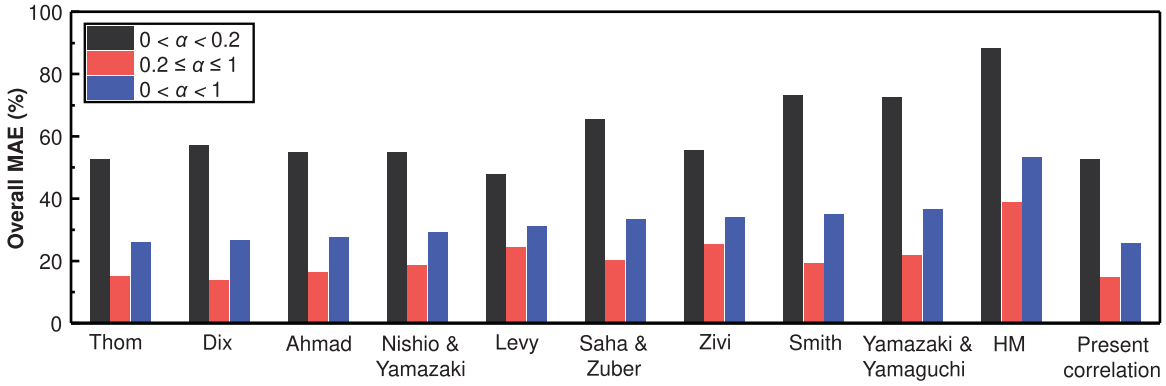

Fig. 4. Mean absolute errors for different void fraction models and correlations segregated relative to two ranges of void fraction.

tenable. Second, possible sources of large MAE are associated with the measurement of void fraction because of both sensor and data processing errors; those are reflected in appreciable data scatter in certain experimental works. Furthermore, as discussed earlier, most void fraction predictive methods, including the present, are based on the assumption that vapor generation will commence at the NVG point, essentially neglecting contribution of the region upstream of NVG corresponding to very small (near zero) void fraction. Also, given both the very small values of both predicted and measured void fractions shortly downstream of the NVG point, and increased uncertainty of measurements in the same region, errors are generally magnified for low void fractions.

To further explore the significance of these errors, MAEs for the same models and correlations presented in Fig. 3 are segregated in Fig. 4 into two separate void fraction ranges: low range (associated with high measurement errors) of $0 < \alpha < 0.2$, and higher range of $0.2 \leq \alpha \leq 1$; also shown are the overall MAE values for the entire range of $0 < \alpha < 1$. Notice how, for all models and correlations, MAE values for $0 < \alpha < 0.2$ are considerably higher than those for $0.2 \leq \alpha \leq 1$. Interestingly, the MAEs for $0.2 \leq \alpha \leq 1$ are reduced considerably compared to the overall values for $0 < \alpha < 1$: from 25.79% to 14.75%, 26.32% to 13.66%, 27.42% to 16.17%, 29.00% to 18.41%, 30.92% to 24.06%, 33.18% to 20.05%, 33.85% to 25.05%, 34.69% to 18.96%, 36.38% to 21.54%, 53.11% to 38.72% for the relations by Thom, Dix, Ahmad, Nishio and Yamazaki, Levy, Saha and Zuber, Zivi, Smith, Yamazaki and Yamaguchi, and according to the homogenous model, respectively. Overall, considering only data in the range of $0.2 \leq \alpha \leq 1$, best predictions are achieved with the relation by Dix followed by Thom's (notice the order of lowest MAE of the two is reversed compared to Fig. 3), evidenced by their smallest MAEs of 13.66% and 14.75%, respectively. However, one disadvantage of the Dix model is that predicts a void fraction smaller than unity for $x = 1$, especially in cases of high inlet pressure and low mass velocity, which is why Thom's method is preferred among all previous predictive methods. Notice also in Fig. 4 that, with MAEs of 52.58%, 14.59% and 25.59% for $0 < \alpha < 0.2$, $0.2 \leq \alpha \leq 1$ and $0 < \alpha < 1$, respectively, the new correlation, Eq. (9), surpasses those of Thom and Dix in predictive accuracy for all void fraction ranges excepting Dix's $0.2 \leq \alpha \leq 1$ range.

6.4. Recommended procedure for calculating void fraction

After the detailed assessment of 16, 4 and 49 models and correlations used to predict $x_e|_{NVG}$, x and α, respectively, against the present consolidated database, a void fraction calculation procedure yielding the highest overall accuracy is recommended and summarized in Fig. 5.

As can be concluded from the previous sections, despite the successes of several models and correlations at predicting $x_e|_{NVG}$, x and α, determining void fraction for subcooled flow boiling remains quite challenging and warrants significant future work. Recommended efforts include:

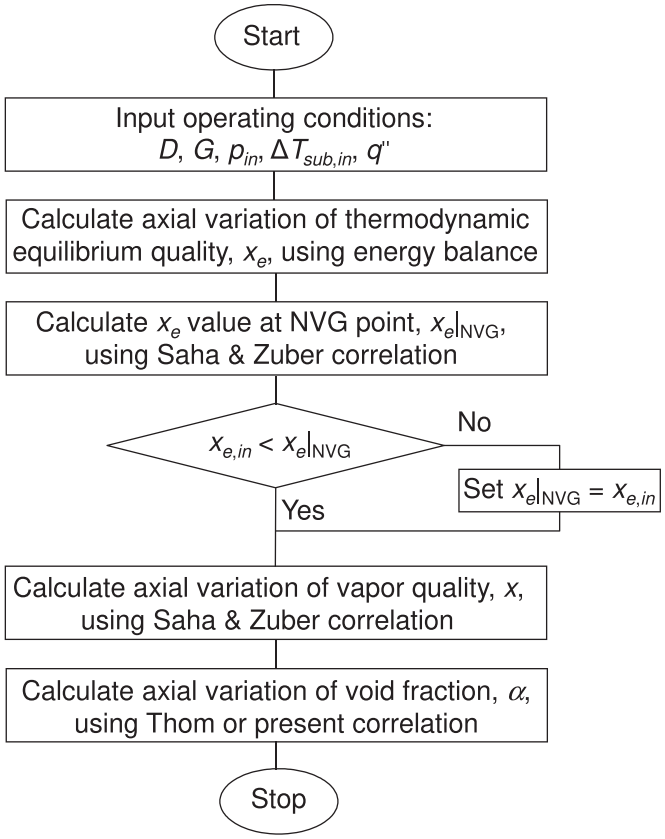

Fig. 5. Recommended procedure for calculating the void fraction.

1. Developing more accurate and robust instrumentation and data processing methods for measurement of low void fraction.
2. Performing void fraction measurements for subcooled boiling in vertical upflow for a multitude of fluids.
3. Performing void fraction measurements for subcooled boiling in different flow orientations, given the appreciable influence of orientation on interfacial behavior and, therefore, void fraction in tubes [130,131].
4. Capitalize of the successes of recent theoretical and computational modeling tools, which have shown significant successes in modeling interfacial behavior in both boiling [132] and con-

densing [133,134] flows to provide a more systematic basis for predicting void fraction.

7. Concluding remarks

This paper includes a review and assessment of the accuracy of prior models and correlations for net vapor generation point, vapor quality, and void fraction in subcooled vertical upflow boiling in a circular tube. Also discussed are the rationale and physical mechanisms upon which the individual predictive methods are based. The assessment is based on a new consolidated database consisting of 61 data points for thermodynamic equilibrium quality at the net vapor generation point, amassed from 5 sources, and 1118 data points for void fraction, from 11 sources. Following are key conclusions from the study:

(1) Despite some successes in predicting the point of net vapor generation, the mechanism of initiating significant vapor generation is not well understood. Best predictions of the point of net vapor generation over the entire range of operating conditions are achieved with a correlation by Saha and Zuber.
(2) Axial distribution of vapor quality in the subcooled region has generally been accomplished using both empirical and mechanistic formulations. Here too, a correlation by Saha and Zuber provides best overall predictive accuracy.
(3) In terms of void fraction prediction, best accuracy among prior predictive methods is achieved, in order, using a slip ratio model by Thom, drift-flux model by Dix, slip ratio model by Ahmad, and modified homogeneous model by Nishino and Yamazaki. And far better accuracy is achieved by the vast majority of the models and correlations over the higher range of void fraction of 0.20-1.0 than the low range of 0-0.2.
(4) A new and simple void fraction correlation spanning the entire range of flow conditions of the consolidated database is proposed, which is shown to yield superior overall predictive accuracy compared to prior models and correlations, and a step-by-step procedure for calculating void fraction with best accuracy is recommended.

Declaration of Competing Interest

The authors declare that there are no conflicts of interest.

Acknowledgments

Financial support from National Natural Science Foundation of China (grant no. 51936002) and China Scholarship Council (grant no. 201806060070) is gratefully acknowledged.

References

[1] Y. Gao, S. Shao, H. Xu, H. Zou, M. Tang, C. Tian, Numerical investigation on onset of significant void during water subcooled flow boiling, Appl. Therm. Eng. 105 (2016) 8–17.
[2] I. Mudawar, Recent advances in high-flux, two-phase thermal management, J. Therm. Sci. Eng. Appl. 5 (2013) 021012.
[3] T.J. LaClair, I. Mudawar, Thermal transients in a capillary evaporator prior to the initiation of boiling, Int. J. Heat Mass Transfer 43 (2000) 3937–3952.
[4] I. Mudawar, T.M. Anderson, Parametric investigation into the effects of pressure, subcooling, surface augmentation and choice of coolant on pool boiling in the design of cooling systems for high-power density chips, J. Electron. Packag. 112 (1990) 375–382.
[5] M.E. Johns, I. Mudawar, An ultra-high power two-phase jet-impingement avionic clamshell module, J. Electron. Packag. 118 (1996) 264–270.
[6] W.P. Klinzing, J.C. Rozzi, I. Mudawar, Film and transition boiling correlations for quenching of hot surfaces with water sprays, J. Heat Treating 9 (1992) 91–103.
[7] S. Mukherjee, I. Mudawar, Pumpless loop for narrow channel and micro-channel boiling from vertical surfaces, J. Electron. Packag. 125 (2003) 431–441.
[8] I. Mudawar, Two-phase micro-channel heat sinks: theory, applications and limitations, J. Electron. Packag. 133 (2011) 041002-2.
[9] O.S. Al-Yahia, D. Jo, ONB, OSV, and OFI for subcooled flow boiling through a narrow rectangular channel heated on one-side, Int. J. Heat Mass Transfer 116 (2018) 136–151.
[10] H. Qian, P. Hrnjak, Void fraction measurement and flow regimes visualization of R134a in horizontal and vertical ID 7 mm circular tubes, Int. J. Refrig. 103 (2019) 191–203.
[11] H.M. Prasser, M. Misawa, I. Tiseanu, Comparison between wire-mesh sensor and ultra-fast X-ray tomograph for an air–water flow in a vertical pipe, Flow Meas. Instrum. 16 (2005) 73–83.
[12] R.E. Vieira, N.R. Kesana, C.F. Torres, B.S. McLaury, S.A. Shirazi, E. Schleicher, U. Hampel, Experimental investigation of horizontal gas–liquid stratified and annular flow using wire-mesh sensor, J. Fluids Eng. 136 (2014) 121301.
[13] J.W. Berthold, S.E. Reed, C.A. Nash, Fibre optic sensor system for void fraction measurement in aqueous two-phase fluids, Flow Meas. Instrum. 5 (1994) 3–13.
[14] D. Morris, A. Teyssedou, J. Lapierre, A. Tapucu, Optical fiber probe to measure local void fraction profiles, Appl. Optics 26 (1987) 4660–4664.
[15] F. Devia, M. Fossa, Design and optimisation of impedance probes for void fraction measurements, Flow Meas. Instrum. 14 (2003) 139–149.
[16] M. Rocha, J.R. Simões-Moreira, Void fraction measurement and signal analysis from multiple-electrode impedance sensors, Heat Transfer Eng 29 (2008) 924–935.
[17] A. Iskandrani, G. Kojasoy, Local void fraction and velocity field description in horizontal bubbly flow, Nucl. Eng. Des. 204 (2001) 117–128.
[18] R. Srisomba, O. Mahian, A.S. Dalkilic, S. Wongwises, Measurement of the void fraction of R-134a flowing through a horizontal tube, Int. Comm. Heat Mass Transfer 56 (2014) 8–14.
[19] S. Wongwises, M. Pipathattakul, Flow pattern, pressure drop and void fraction of two-phase gas–liquid flow in an inclined narrow annular channel, Exp. Therm. Fluid Sci. 30 (2006) 345–354.
[20] H.-M. Liu, T.-K. Wang, A modified one-shot photon-attenuation method for void fraction determination in two-phase-flow systems, Int. J. Rad. Appl. Instrum. A 42 (1991) 25–30.
[21] H. Asano, N. Takenaka, T. Fujii, Flow characteristics of gas–liquid two-phase flow in plate heat exchanger:(Visualization and void fraction measurement by neutron radiography), Exp. Therm. Fluid Sci. 28 (2004) 223–230.
[22] S. Jahangir, E.C. Wagner, R.F. Mudde, C. Poelma, Void fraction measurements in partial cavitation regimes by X-ray computed tomography, Int. J. Multiph. Flow 120 (2019) 103085.
[23] G.H. Roshani, E. Nazemi, S.A.H. Feghhi, S. Setayeshi, Flow regime identification and void fraction prediction in two-phase flows based on gamma ray attenuation, Measurement 62 (2015) 25–32.
[24] E. Nazemi, S.A.H. Feghhi, G.H. Roshani, R. Gholipour Peyvandi, S. Setayeshi, Precise void fraction measurement in two-phase flows independent of the flow regime using gamma-ray attenuation, Nucl. Eng. Technol. 48 (2016) 64–71.
[25] H. Murakawa, H. Kikura, M. Aritomi, Application of ultrasonic Doppler method for bubbly flow measurement using two ultrasonic frequencies, Exp. Therm. Fluid Sci. 29 (2005) 843–850.
[26] Y. Murai, S. Ohta, A. Shigetomi, Y. Tasaka, Y. Takeda, Development of an ultrasonic void fraction profiler, Meas. Sci. Technol. 20 (2009) 114003.
[27] K. De Kerpel, B. Ameel, C. T'Joen, H. Canière, M. De Paepe, Flow regime based calibration of a capacitive void fraction sensor for small diameter tubes, Int. J. Refrig. 36 (2013) 390–401.
[28] K. De Kerpel, B. Ameel, S. De Schampheleire, C. T'Joen, H. Canière, M. De Paepe, Calibration of a capacitive void fraction sensor for small diameter tubes based on capacitive signal features, Appl. Therm. Eng. 63 (2014) 77–83.
[29] M.V. Sardeshpande, S. Harinarayan, V.V. Ranade, Void fraction measurement using electrical capacitance tomography and high speed photography, Chem. Eng. Res. Des. 94 (2015) 1–11.
[30] Y. Sakamoto, H. Kobayashi, Y. Naruo, Y. Takesaki, Y. Nakajima, A. Furuichi, H. Tsujimura, K. Kabayama, T. Sato, Investigation of the void fraction–quality correlations for two-phase hydrogen flow based on the capacitive void fraction measurement, Int. J. Hydrogen Energy 44 (2019) 18483–18495.
[31] J.X.F. Ribeiro, R. Liao, A.M. Aliyu, Y.D. Baba, A. Archibong-Eso, A. Ehinmowo, L. Zilong, An assessment of gas void fraction prediction models in highly viscous liquid and gas two-phase vertical flows, J. Natural Gas Sci. Eng. 76 (2020) 103107.
[32] P.V. Godbole, Study of Flow Patterns and Void Fraction in Vertical Upward Two-Phase Flow, Oklahoma State University, 2009.
[33] M.A. Woldesemayat, A.J. Ghajar, Comparison of void fraction correlations for different flow patterns in horizontal and upward inclined pipes, Int. J. Multiph. Flow 33 (2007) 347–370.
[34] P.V. Godbole, C.C. Tang, A.J. Ghajar, Comparison of void fraction correlations for different flow patterns in upward vertical two-phase flow, Heat Transfer Eng. 32 (2011) 843–860.
[35] F. Kaminaga, Assessment of void fraction correlations for vertical two-phase flow in small diameter tube at low liquid velocity, J. Nucl. Sci. Technol. 29 (1992) 695–698.

[36] D. Maier, Review of wide range void correlations of against and extensive data base of rod bundle void measurements, in: Proc. of 5th International Conference on Nuclear Engineering (ICONE-5), May 26-30, Nice, France, 1997.
[37] A. Inoue, T. Kurosu, M. Yagi, S. Morooka, A. Hoshide, T. Ishizuka, K. Yoshimura, In-bundle void measurement of a BWR fuel assembly by an X-ray CT scanner: assessment of BWR design void correlation and development of new void correlation, in: Proc. of the ASME/JSME Nuclear Engineering Conference, 1993.
[38] M. Sadatomi, K. Kano, A. Kawahara, N. Mori, Void fraction and pressure drop in two-phase equilibrium flows in a vertical 2×3 rod bundle channel–assessment of correlations against the present subchannel data, JSME Int. J. Series B: Fluids Therm. Eng. 49 (2006) 279–286.
[39] R. Diener, L. Friedel, Reproductive accuracy of selected void fraction correlations for horizontal and vertical upflow, Forsch. Ingenieurwes. 64 (1998) 87–97.
[40] S.M. Bhagwat, A.J. Ghajar, Similarities and differences in the flow patterns and void fraction in vertical upward and downward two phase flow, Exp. Therm. Fluid Sci. 39 (2012) 213–227.
[41] Y. Xu, X. Fang, Correlations of void fraction for two-phase refrigerant flow in pipes, Appl. Therm. Eng. 64 (2014) 242–251.
[42] P. Coddington, R. Macian, A study of the performance of void fraction correlations used in the context of drift-flux two-phase flow models, Nucl. Eng. Des. 215 (2002) 199–216.
[43] A. Cioncolini, J.R. Thome, Void fraction prediction in annular two-phase flow, Int. J. Multip. Flow 43 (2012) 72–84.
[44] B. Chexal, J. Horowitz, G. Lellouche, An assessment of eight void fraction models, Heat Transfer: Pittsburgh (1987).
[45] P.K. Vijayan, N. Maruthi Ramesh, D.S. Pilkhwal, D. Saha, An Assessment of Void Fraction Correlations for Vertical Upward Steam-Water Flow, Bhabha Atomic Research Centre, 1997.
[46] P.K. Vijayan, A.P. Patil, D.S. Pilkhwal, D. Saha, V.V. Raj, An assessment of pressure drop and void fraction correlations with data from two-phase natural circulation loops, Heat Mass Transfer 36 (2000) 541–548.
[47] P.G. Kroeger, N. Zuber, An analysis of the effects of various parameters on the average void fractions in subcooled boiling, Int. J. Heat Mass Transfer 11 (1968) 211–233.
[48] P. Griffith, J.A. Clark, W.M. Rohsenow, Void volumes in subcooled boiling systems, ASME Paper 58-HT-19, U.S. National Heat Transfer Conference, 1958.
[49] S.Y. Ahmad, Axial distribution of bulk temperature and void fraction in a heated channel with inlet subcooling, ASME J. Heat Transfer 92 (1970) 595–609.
[50] P. Saha, N. Zuber, Point of net vapor generation and vapor void fraction in subcooled boiling, in: International Heat Transfer Conference Digital Library, 4, 1974, pp. 175–179.
[51] H.C. Ünal, Determination of the initial point of net vapor generation in flow boiling systems, Int. J. Heat Mass Transfer 18 (1975) 1095–1099.
[52] O.M. Zeitoun, Subcooled Flow Boiling and Condensation, McMaster University, Hamilton, ON, 1994.
[53] R. Ahmadi, T. Okawa, Recognition of net vapor generation in subcooled flow boiling, J. Multidisciplinary Eng. Sci. Technol. 2 (2015) 465–469.
[54] S.C. Lee, S.G. Bankoff, A comparison of predictive models for the onset of significant void at low pressures in forced-convection subcooled boiling, KSME Int. J. 12 (1998) 504–513.
[55] K.S. Ha, Y.B. Lee, H.C. No, Improvements in predicting void fraction in subcooled boiling, Nucl. Technol. 150 (2005) 283–292.
[56] T.W. Ha, J.J. Jeong, B. Yun, H.Y. Yoon, Improvement of the MARS subcooled boiling model for low-pressure, low-Pe flow conditions, Ann. Nucl. Energy 120 (2018) 236–245.
[57] T.-W. Ha, J.J. Jeong, B.-J. Yun, Improvement of the MARS subcooled boiling model for a vertical upward flow, Nucl. Eng. Technol. 51 (2019) 977–986.
[58] T.-W. Ha, B.-J. Yun, J.J. Jeong, Improvement of the subcooled boiling model for thermal–hydraulic system codes, Nucl. Eng. Des. 364 (2020) 110641.
[59] S. Levy, Forced convection subcooled boiling—prediction of vapor volumetric fraction, Int. J. Heat Mass Transfer 10 (1967) 951–965.
[60] J.T. Rogers, M. Salcudean, Z. Abdullah, D. McLeod, D. Poirier, The onset of significant void in up-flow boiling of water at low pressure and velocities, Int. J. Heat Mass Transfer 30 (1987) 2247–2260.
[61] J. Li, The Onset of Significant Void in Boiling Flows Over a Wide Range Of Operation Conditions, Carleton University, 1992.
[62] F.W. Staub, The void fraction in subcooled boiling—prediction of the initial point of net vapor generation, J. Heat Transfer 90 (1968) 151–157.
[63] R. Hino, T. Ueda, Studies on heat transfer and flow characteristics in subcooled flow boiling—Part 1. Boiling characteristics, Int. J. Multiph. Flow 11 (1985) 269–281.
[64] E.L. Bibeau, M. Salcudean, Subcooled void growth mechanisms and prediction at low pressure and low velocity, Int. J. Multiph. Flow 20 (1994) 837–863.
[65] M.D. Bartel, M. Ishii, T. Masukawa, Y. Mi, R. Situ, Interfacial area measurements in subcooled flow boiling, Nucl. Eng. Des. 210 (2001) 135–155.
[66] G.E. Dix, Vapor Void Fractions for Forced Convection with Subcooled Boiling at Low Flow Rates Ph.D. Thesis, University of California, 1971.
[67] J.G. Collier, J.R. Thome, Convective Boiling and Condensation, Clarendon Press, 1994.
[68] P.K. Jain, K. Nourmohammadi, R.P. Roy, A study of forced convective subcooled boiling in heated annular channels, Nucl. Eng. Des. 60 (1980) 401–411.
[69] K. Sekoguchi, O. Tanaka, S. Esaki, T. Imasaka, Prediction of void fraction in subcooled and low quality boiling regions, Bull. JSME 23 (1980) 1475–1482.
[70] M. Siman-Tov, D. Felde, J.L. McDuffee, G.L. Yoder, Experimental Study of Static Flow Instability in Subcooled Flow Boiling in Parallel Channels, Oak Ridge National Lab., TN (United States), 1995.
[71] I. Kataoka, S. Kodama, A. Tomiyama, A. Serizawa, Study on analytical prediction of forced convective CHF based on multi-fluid model, Nucl. Eng. Des. 175 (1997) 107–117.
[72] V. Kalitvianski, Qualification of CATHARE 2 V1. 5 Rev. 6 on Subcooled Boiling Experiments (KIT tests), CEA, Grenoble, France, 2000 Technical Report.
[73] Q. Sun, R. Yang, H. Zhao, Predictive study of the incipient point of net vapor generation in low-flow subcooled boiling, Nucl. Eng. Des. 225 (2003) 249–256.
[74] N. Zuber, J. Findlay, Average volumetric concentration in two-phase flow systems, J. Heat Transfer 87 (1965) 453–468.
[75] S. Levy, Steam slip—theoretical prediction from momentum model, J. Heat Transfer 82 (1960) 113–124.
[76] Y. Yamazaki, K. Yamaguchi, Vold fraction correlation for boiling and non-boiling vertical two-phase flows in tube, J. Nucl. Sci. Technol. 13 (1976) 701–707.
[77] J.C. Lai, B. Farouk, Numerical simulation of subcooled boiling and heat transfer in vertical ducts, Int. J. Heat Mass Transfer 36 (1993) 1541–1551.
[78] E. Krepper, B. Končar, Y. Egorov, CFD modelling of subcooled boiling—concept, validation and application to fuel assembly design, Nucl. Eng. Des. 237 (2007) 716–731.
[79] J.Y. Tu, G.H. Yeoh, On numerical modelling of low-pressure subcooled boiling flows, Int. J. Heat Mass Transfer 45 (2002) 1197–1209.
[80] S. Sivalingam, S.S. Paramanantham, W.-G. Park, Numerical simulation of vapor volume fraction in a vertical channel under low-pressure conditions, J. Mechanical Sci. Technol. 32 (2018) 4657–4664.
[81] T. Okawa, H. Kubota, T. Ishida, Simultaneous measurement of void fraction and fundamental bubble parameters in subcooled flow boiling, Nucl. Eng. Des. 237 (2007) 1016–1024.
[82] S. Hari, Y.A. Hassan, Improvement of the subcooled boiling model for low–pressure conditions in thermal-hydraulic codes, Nucl. Eng. Des. 216 (2002) 139–152.
[83] A.A. Armand, G.G. Treščev, Investigation of the resistance during the movement of steam-water mixtures in a heated boiler pipe at high pressure, Atomic Energy Res. Establishment (1959).
[84] S.G. Bankoff, A variable density single-fluid model for two-phase flow with particular reference to steam-water flow, J. Heat Transfer 82 (1960) 265–272.
[85] W. Massena, Steam-Water Pressure Drop and Critical Discharge Flow-a Digital Computer Program, General Electric Co. Hanford Atomic Products Operation, Richland, Wash., 1960.
[86] A.B. Jones, Hydrodynamic Stability of a Boiling Channel, Knolls Atomic Power Lab., Schenectady, NY, 1961.
[87] H. Nishino, Y. Yamazaki, A new method of evaluating steam volume fractions in boiling systems, J. Soc. Atom. Energy Jpn. 5 (1963) 39–59.
[88] D. Chisholm, Two-Phase Flow in Pipelines and Heat Exchangers, George Godwin London, 1983.
[89] G.W. Maurer, A method of predicting steady-state boiling vapor fractions in reactor coolant channels, Bettis Technical Review, WAPD-BT-19, (1960) 59-70.
[90] H. Fauske, Critical two-phase, steam–water flows, in: Proceedings of the 1961 Heat Transfer and Fluid Mechanics Institute, Stanford, CA, Stanford University Press, 1961, pp. 79–89.
[91] J.R.S. Thom, Prediction of pressure drop during forced circulation boiling of water, Int. J. Heat Mass Transfer 7 (1964) 709–724.
[92] D. Butterworth, A comparison of some void-fraction relationships for co-current gas-liquid flow, Int. J. Multiph. Flow 1 (1975) 845–850.
[93] S.M. Zivi, Estimation of steady-state steam void-fraction by means of the principle of minimum entropy production, J. Heat Transfer 86 (1964) 247–252.
[94] J.M. Turner, G.B. Wallis, The separate-cylinders model of two-phase flow, Paper No. NYO-3114-6, Thayer's School Engineering, Dartmouth College, Hanover, NH, USA, 1965.
[95] S.L. Smith, Void fractions in two-phase flow: a correlation based upon an equal velocity head model, Proc. Inst. Mech. Eng. 184 (1969) 647–664.
[96] G.B. Wallis, One-Dimensional Two-Phase Flow, McGraw-Hill, New York, 1969.
[97] D. Chisholm, Pressure gradients due to friction during the flow of evaporating two-phase mixtures in smooth tubes and channels, Int. J. Heat Mass Transfer 16 (1973) 347–358.
[98] N. Madsen, A void fraction correlation for vertical and horizontal bulk-boiling of water, AIChE J. 21 (1975) 607–608.
[99] P.L. Spedding, J.J.J. Chen, Correlation and estimation of holdup in two-phase flow, in: Proceedings of N. Z. Geothermal Workshop, 1979, pp. 180–199.
[100] J.J.J. Chen, P.L. Spedding, An extension of the Lockhart-Martinelli theory of two phase pressure drop and holdup, Int. J. Multiph. Flow 7 (1981) 659–675.
[101] J.J.J. Chen, A further examination of void fraction in annular two-phase flow, Int. J. Heat Mass Transfer 29 (1986) 1760–1763.
[102] A. Khalil, G. McIntosh, R.W. Boom, Experimental measurement of void fraction in cryogenic two phase upward flow, Cryogenics 21 (1981) 411–414.
[103] R.H.S. Winterton, Thermal Design of Nuclear Reactors, Pergamon Press, Oxford, 2014.
[104] D.J. Nicklin, Two-phase flow in vertical tubes, Inst. Chem. Eng. 40 (1962) 61–68.
[105] S.Z. Rouhani, E. Axelsson, Calculation of void volume fraction in the subcooled and quality boiling regions, Int. J. Heat Mass Transfer 13 (1970) 383–393.
[106] M. Ishii, One-Dimensional Drift-Flux Model and Constitutive Equations for Relative Motion Between Phases in Various Two-Phase Flow Regimes, Argonne National Lab., Ill.(USA), 1977.

[107] H.C. Ünal, Void fraction and incipient point of boiling during the subcooled nucleate flow boiling of water, Int. J. Heat Mass Transfer 20 (1977) 409–419.
[108] H.C. Ünal, Determination of the drift velocity and the void fraction for the bubble-and plug-flow regimes during the flow boiling of water at elevated pressures, Int. J. Heat Mass Transfer 21 (1978) 1049–1056.
[109] K.H. Sun, R.B. Duffey, C.M. Peng, The prediction of two-phase mixture level and hydrodynamically-controlled dryout under low flow conditions, Int. J. Multiph. Flow 7 (1981) 521–543.
[110] H.G. Sonnenburg, Full-range drift-flux model based on the combination of drift-flux theory with envelope theory, in: Proceedings of 4th International Topical Meeting on Nuclear Reactor Thermal-hydraulics, Karlsruhe, Germany, 1989, pp. 1003–1009.
[111] D. Bestion, The physical closure laws in the CATHARE code, Nucl. Eng. Des. 124 (1990) 229–245.
[112] G.C. Gardner, Fractional vapour content of a liquid pool through which vapour is bubbled, Int. J. Multiph. Flow 6 (1980) 399–410.
[113] T.N. Tandon, H.K. Varma, C.P. Gupta, A void fraction model for annular two-phase flow, Int. J. Heat Mass Transfer 28 (1985) 191–198.
[114] R. Huq, J.L. Loth, Analytical two-phase flow void prediction method, J. Thermo Phys. 6 (1992) 139–144.
[115] H.S. Isbin, D. Biddle, Void-fraction relationships for upward flow of saturated, steam-water mixtures, Int. J. Multiph. Flow 5 (1979) 293–299.
[116] J.M. Delhaye, F. Maugin, J.M. Ochterbeck, Void fraction predictions in forced convective subcooled boiling of water between 10 and 18 MPa, Int. J. Heat Mass Transfer 47 (2004) 4415–4425.
[117] J.K. Ferrell, A study of convection boiling inside channels, Raleigh, North Carolina, 1964.
[118] G.G. Bartolomei, V.M. Chanturiya, Experimental study of true void fraction when boiling subcooled water in vertical tubes, Therm. Eng. 14 (1967) 123–128.
[119] Z. Edelman, E. Elias, Void fraction distribution in low flow rate subcooled boiling, Nucl. Eng. Des. 66 (1981) 375–382.
[120] G.G. Bartolomei, V.G. Brantov, Y.S. Molochnikov, Y.V. Kharitonov, V.A. Solodkii, G.N. Batashova, V.N. Mikhailov, An experimental investigation of true volumetric vapor content with subcooled boiling in tubes, Therm. Eng. 29 (1982) 132–135.
[121] D.A. Labuntsov, A.G. Lobachev, B.A. Kolchugin, E.A. Zakharova, The main principles of variation in vapor content of equilibrium and non-equilibrium 2-phase flows in channels of different geometry, Therm. Eng. 31 (1984) 506–508.
[122] S.Z. Rouhani, K.M. Becker, Measurement of void fraction for flow of boiling heavy water in vertical round ducts, Aktebolaget Atomenergie Rep. (1963).
[123] J.R.S. Thom, W.M. Walker, T.A. Fallon, G.F.S. Reising, Boiling in sub-cooled water during flow up heated tubes or annuli, Spitzer Proposal 3 (1967) 226–246.
[124] K.K. Fung, D.C. Groeneveld, Measurement of void fraction in steady-state subcooled and low quality flow film boiling, Int. J. Multiph. Flow 6 (1980) 357–361.
[125] G.R. Dimmick, W.N. Selander, A dynamic model for predicting subcooled void: experimental results and model development, EUROTHERM Seminar #16, 1990.
[126] P.S. Larsen, L.S. Tong, Void fractions in subcooled flow boiling, J. Heat Transfer 91 (1969) 471–476.
[127] A.S. Devkin, A.S. Podosenov, RELAP5/MOD3 Subcooled Boiling Model Assessment, U.S. Nuclear Regulatory Commission, United States, 1998.
[128] NISTStandard Reference Database-REFPROP Version 8.0, National Institute of Standard and Technology, Boulder, Colorado, 2007.
[129] B. Chexal, G. Lellouche, J. Horowitz, J. Healzer, A void fraction correlation for generalized applications, Progr. Nucl. Energy 27 (1992) 255–295.
[130] H. Zhang, I. Mudawar, M.M. Hasan, Experimental and theoretical study of orientation effects on flow boiling CHF, Int. J. Heat Mass Transfer 45 (2002) 4463–4478.
[131] C. Konishi, I. Mudawar, Review of flow boiling and critical heat flux in microgravity, Int. J. Heat Mass Transfer 80 (2015) 469–493.
[132] S.M. Kim, I. Mudawar, Universal approach to predicting saturated flow boiling heat transfer in mini/micro-channels part I. Dryout incipience quality, Int. J. Heat Mass Transfer 64 (2013) 1226–1238.
[133] S.M. Kim, I. Mudawar, Theoretical model for annular flow condensation in rectangular micro-channels, Int. J. Heat Mass Transfer 55 (2012) 958–970.
[134] H. Lee, C.R. Kharangate, N. Mascarenhas, I. Park, I. Mudawar, 2015 I., Experimental and computational investigation of vertical downflow condensation, Int. J. Heat Mass Transfer 85 (2015) 865–879.